SPLICE RESEARCH
Progress Report
ANALYTICAL AND EXPERIMENTAL INVESTIGATION OF THE MULTIPLE ROW EXTENDED 1/3 MOMENT END-PLATE CONNECTION WITH EIGHT BOLTS AT THE BEAM TENSION FLANGE

by
Scott J. Morrison
and
Abolhassan Astaneh-Asl
Thomas M. Murray
Co-Principal Investigators

Sponsored by
Metal Building Manufacturers Association
and
American Institute of Steel Construction

Report No. FSEL/MBMA 86-01

May 1986

FEARS STRUCTURAL ENGINEERING LABORATORY
School of Civil Engineering and Environmental Science
University of Oklahoma
Norman, Oklahoma 73019

TABLE OF CONTENTS

LIST OF FIGURES

ANALYTICAL AND EXPERIMENTAL INVESTIGATION
OF THE MULTIPLE ROW EXTENDED 1/3 MOMENT END-PLATE CONNECTION
WITH EIGHT BOLTS AT THE BEAM TENSION FLANGE

CHAPTER I

INTRODUCTION

1.1 Background

Moment end-plate connections are commonly used in steel portal frame construction as bolted moment-resistant connections. The moment end-plate is typically used to connect a beam to a beam, often referred to as a "splice-plate connection", Figure 1.1(a), or to connect a beam to a column, Figure 1.1(b).

Several design procedures for various moment end-plate configurations have been suggested to determine end-plate thickness and bolt diameter based on results from finite-element method, yield-line theory, or experimental test data. Unfortunately, these procedures produce a variety of values for end-plate thickness and bolt diameter for the same design example. For one particular configuration and loading, the variance of design end-plate thickness exceeded 100% [1]. An even greater variation was found for bolt force prediction, as some methods assume prying action is negligible, whereas other methods assume prying action is significant and contributes substantially to bolt force.

Hendrick et al [2] has finalized a unification of design procedures for four configurations of the flush type moment end-plate connection. Two of these flush type connections are unstiffened: the two-bolt unstiffened, Figure 1.2(a), and the four-bolt unstiffened, Figure 1.2(b). The other two flush type connections are stiffened: the four-bolt stiffened with web gusset plate between the two tension bolt rows, Figure 1.2(c), and the four-bolt stiffened with web gusset plate outside the two tension bolt rows, Figure 1.2(d). The gusset plates for each of the flush stiffened connections are symmetrical about the beam web and are welded to the end-plate and the beam web.

Morrison et al [3] has extended the unification of design procedures established by Hendrick et al [2] to a fifth configuration of moment end-plate. This configuration is the four-bolt extended stiffened form shown in Figure 1.3. In this connection, the four bolts in the tension region are placed one row of two bolts on each side of the beam tension flange. A triangular stiffener is located on the end-plate extension outside of the beam depth on the beam web centerline.

This report continues the unification of design procedures for moment end-plate connections established by Hendrick et al [2] and extended by Morrison et at [3] for another configuration of moment end-plate. This sixth configuration is the multiple row extended 1/3 form shown in Figure 1.4. In this connection, the eight bolts in the tension region are placed one row of two bolts outside the depth of the beam and three rows of two bolts inside the depth of the beam. The designation 1/3 reflects the number of bolt rows outside and inside, respectively, the beam depth at the beam tension flange. The unified design procedures include determination of end-plate thickness and prediction of bolt forces.

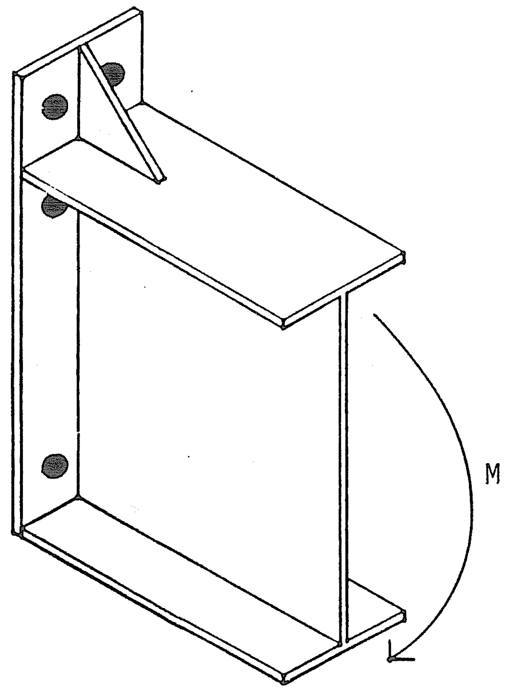

Figure 1.3 Four-Bolt Extended Stiffened Moment End-Plate Connection (Unification Extended by Morrison et al (3))

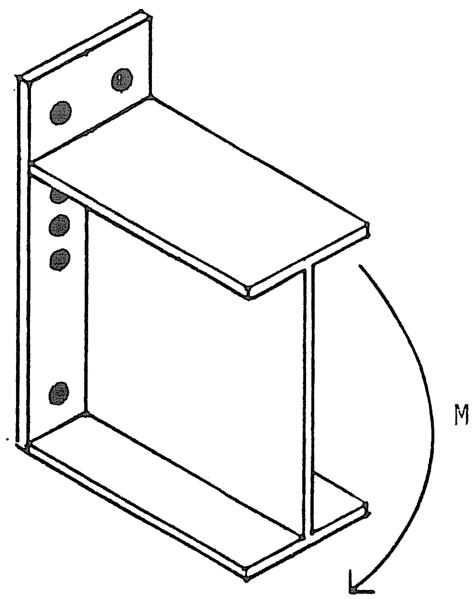

Figure 1.4 Multiple Row Extended 1/3 Moment End-Plate Connection

analytical prediction equations. Figure 1.5 presents the various parameters that define the end-plate geometry. These geometric parameters were varied within the limits shown in Table 1.1 to develop the experimental test matrix.

Table 1.1

Limits of Geometric Parameters

Parameter	Low (in)	Intermediate (in)	High (in)
d_b	3/4	1-1/4	1-1/2
p_f	1-1/8	1-3/4	2-1/2
p_b	2	3-1/2	5
g	2-1/4	3-7/8	5-1/2
h	30	46	62
b_f	6	9	12
t_w	1/4	5/16	3/8
t_f	3/8	5/8	1

CHAPTER II
ANALYTICAL STUDY

2.1 Yield-Line Theory

Yield-lines are the continuous formation of plastic hinges along a straight or curved line. It is assumed that yield-lines divide a plate into rigid plane regions since elastic deformations are negligible when compared with plastic deformations. The failure mechanism of the plate exists when yield-lines form a kinematically valid collapse mechanism. Most of the yield-line theory development is related to reinforced concrete; nonetheless, the principles and findings are also applicable to steel plates.

The analysis of a yield-line mechanism can be performed by two different methods, the equilibrium method and the virtual work or energy method. The latter method is more suitable for the end-plate application and is used herein. In this method, the external work done by the applied load, in moving through a small arbitrary virtual deflection field, is equated to the internal work done as the plate rotates at the yield lines to facilitate this virtual deflection field. For a selected yield-line pattern and loading, a specific plastic moment is required along these hinge lines. For the same loading, other patterns may result in a larger required plastic moment capacity. Hence, the appropriate pattern is that which requires the largest required plastic moment. Conversely, for a given plastic moment capacity, the appropriate mechanism is that which produces the smallest failure load. This implies that the

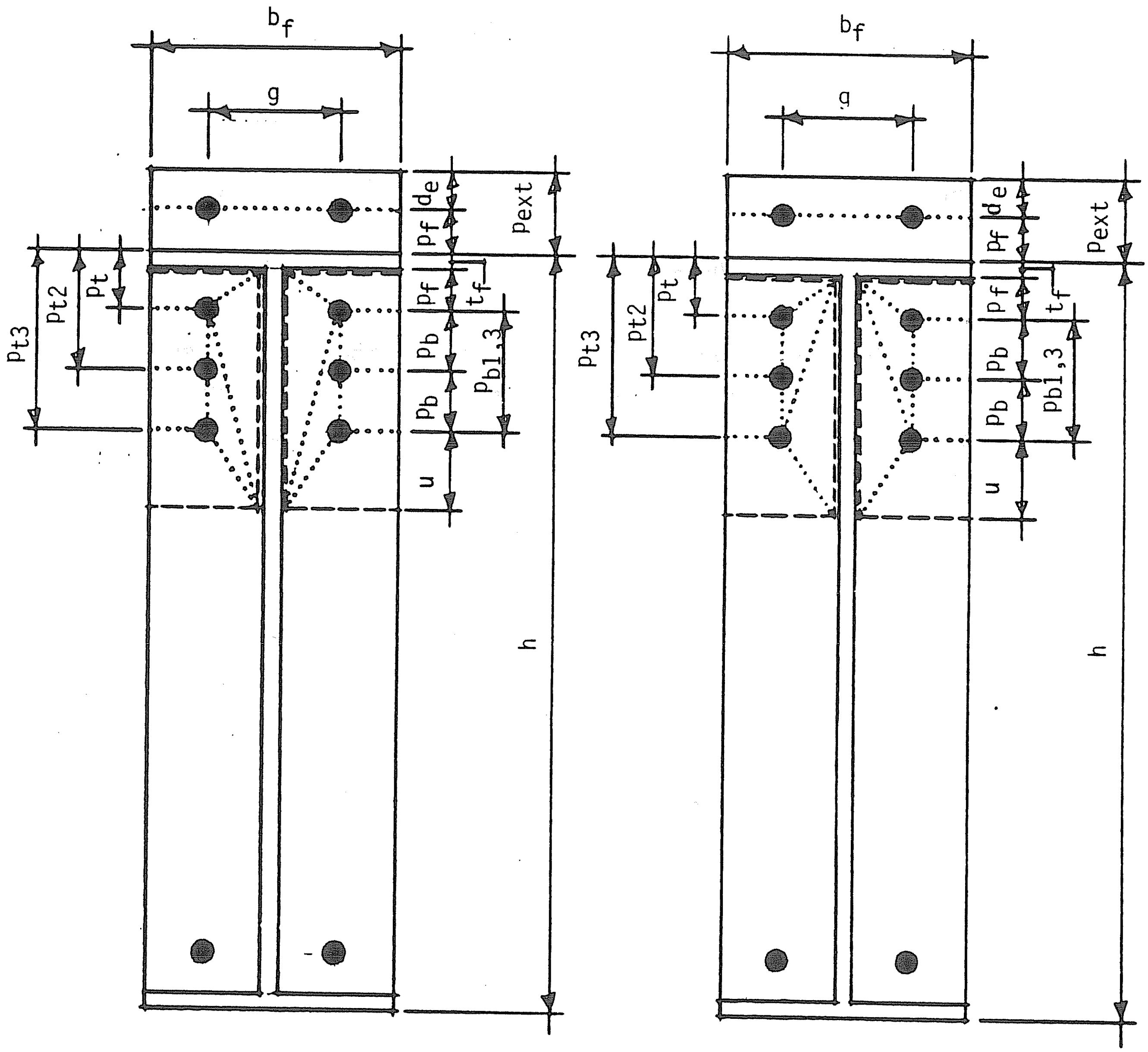

(a) Mechanism 1

(b) Mechanism 2

Figure 2.1 Yield-Line Mechanisms for the Multiple Row Extended 1/3 Moment End-Plate Connection

A photo of an observed yield-line pattern for the multiple row extended 1/3 moment end-plate is shown in Figure 2.2. The yield-line pattern is indicated by the flaking of "white wash" from the test specimen.

2.2 Bolt Force Predictions

Yield-line theory does not produce bolt force predictions including prying action forces. Since experimental results indicate that prying action behavior is present in end-plate connections, a method suggested by Kennedy et al [4] was adopted to predict bolt forces as a function of applied flange force.

The Kennedy method is based on the split-tee analogy and three stages of plate behavior. Consider a split-tee model, Figure 2.3, consisting of a flange bolted to a rigid support and attached to a web through which a tension load is applied. At the lower levels of applied load, the flange behavior is termed thick plate behavior as plastic hinges have not formed in the split-tee flange, Figure 2.4(a). As the applied load is increased, two plastic hinges form at the centerline of the flange and each web face intersection, Figure 2.4(b). This yielding marks the "thick plate limit" and indicates the second stage of plate behavior termed intermediate plate behavior. At a greater applied load level, two additional plastic hinges form at the centerline of the flange and each bolt, Figure 2.4(c). The formation of this second set of plastic hinges marks the "thin plate limit" and indicates the third stage of plate behavior termed thin plate behavior.

For all stages of plate behavior, the Kennedy method predicts a bolt force as the sum of a portion of the applied force and a prying force. The portion of the applied force depends on the applied load, while the magnitude of the

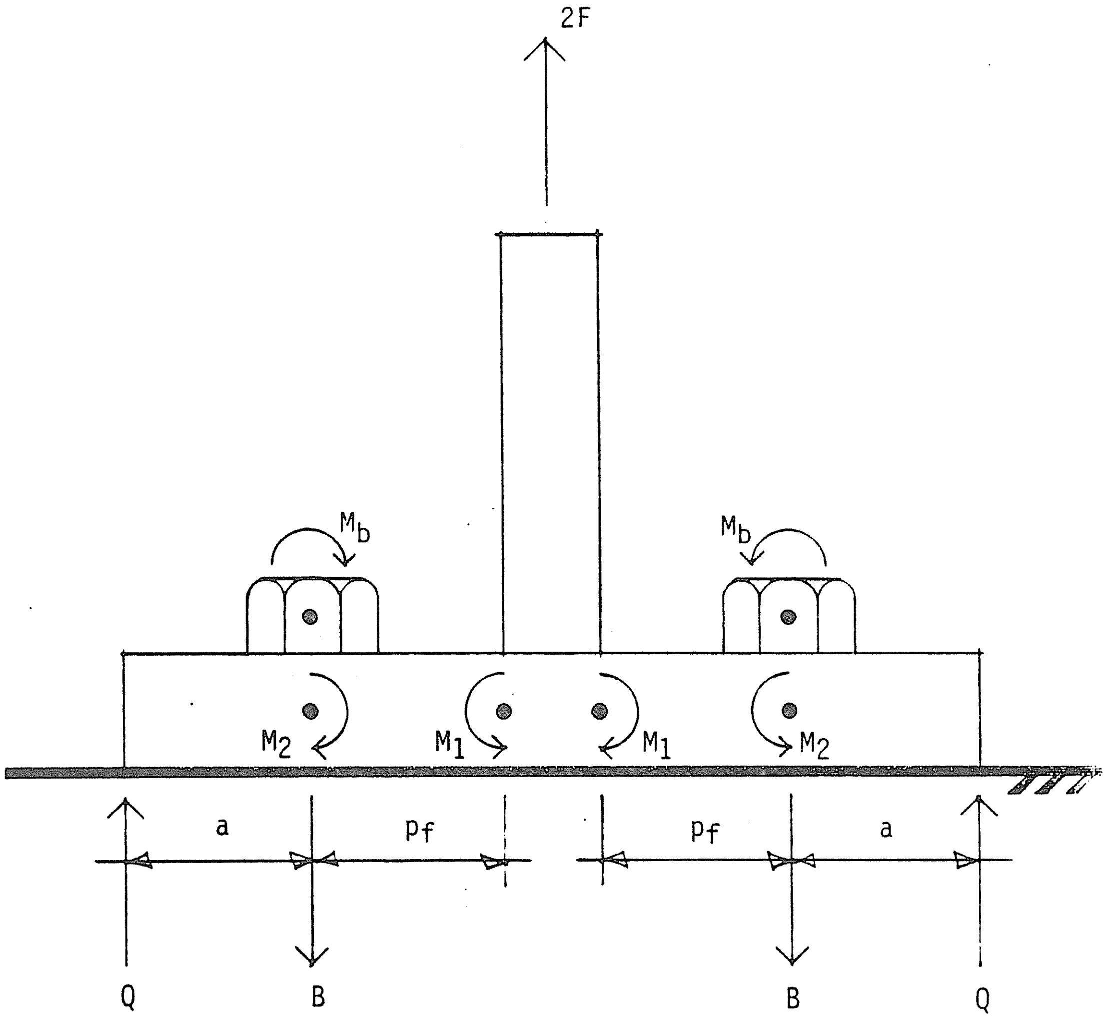

Figure 2.3 Kennedy Method Split-Tee Model

prying force depends on the stage of plate behavior. For the first stage of behavior, or thick plate behavior, the prying force is zero. For the second stage of behavior, or intermediate plate behavior, the prying force increases from zero at the thick plate limit to a maximum at the thin plate limit. For the third stage of behavior, or thin plate behavior, the prying force is maximum and constant. The distance "a" between the point of prying force application and the centerline of bolt has been determined empirically by Hendrick et al [2] for the flush end-plate configurations shown in Figure 1.2, as a function of t_p/d_b:

$$a = 3.682\ (t_p/d_b)^3 - 0.085 \tag{2.7}$$

Modifications of the Kennedy method are necessary for application to the multiple row extended 1/3 moment end-plate connection. First, the connection is idealized in two parts: the outer end-plate and the inner end-plate, Figure 2.5. The outer end-plate consists of the end-plate extension outside the beam tension flange and a portion of the beam tension flange. The inner end-plate consists of the end-plate within the beam flanges and the remaining beam tension flange. Second, four factors: α, β_2, β_3, and β_4, are introduced. These factors proportion the tension flange force to the outer end-plate, the α, and inner end-plate, the β_2, β_3, and β_4. The factors were empirically developed as:

$$\alpha + \beta_2 + \beta_3 + \beta_4 \geq 1.0 \tag{2.8}$$

It was observed in five of six experimental tests (Chapter III) that no contact was made at the outside edges of the two outer end-plates in beam-to-beam connections. Since no contact was made, no prying action is possible. Thus, the outer end-plate behavior is thick at all applied load levels. The outer end-plate bolt force, B_1, is simply the outer flange force, αF_f, divided by the number of outer bolts, 2:

$$B_1 = \alpha F_f / 2 \tag{2.9}$$

The inner end-plate, on the other hand, does exhibit prying action at increased applied load levels in experimental testing. Two of the three inner bolt force are assumed to receive prying force contributions. The bolt force, B_3, not receiving prying force contributions is the second bolt force from the beam tension flange. Since the prying force is zero, the plate behavior is thick at all applied load levels. The bolt force, B_3, is simply a portion of the inner flange force, $\beta_3 F_f$, divided by the number of bolts, 2:

$$B_3 = \beta_3 F_f/2 \tag{2.10}$$

The two bolt forces receiving prying force contributions are the bolt forces nearest to, B_2, and farthest from, B_4, the beam tension flange. In order to determine the magnitudes of these prying forces, and hence, the inner bolt forces, one must first ascertain the stages of inner end-plate behavior. The inner end-plate behavior is established by comparing the appropriate portion of the inner flange force, either $\beta_2 F_f$ or $\beta_4 F_f$, with the flange force at the thick plate limit F_1, and the flange force at the thin plate limit, F_{11}. The flange force at the thick plate limit, F_1, is:

$$F_1 = \frac{b_f t_p{}^2 F_{py}}{4p_f \sqrt{1 + (3t_p{}^2/16p_f{}^2)}} \tag{2.11}$$

The flange force at the thin plate limit, F_{11}, is:

The F' term in the Q_{2max} expression is the lesser of:

$$F_{limit} = F_{11}/2 \qquad (2.17)$$

or

$$F_{2max} = \beta_2 F_f/2 \qquad (2.18)$$

Hence, the inner bolt force, B_2, for thin end-plate behavior is the inner flange force, $\beta_2 F_f$, divided by the number of bolts, 2, plus the prying force, Q_{2max}:

$$B_2 = \beta_2 F_f/2 + Q_{2max} \qquad \text{when } \beta_2 F_f > F_{11} \qquad (2.19)$$

An explanation of bolt force B_4 calculation parallels that for bolt force B_2. Nonetheless, bolt force B_4 equations are presented for completeness:

$$B_4 = \beta_4 F_f/2 \qquad \text{when } \beta_4 F_f < F_1 \qquad (2.20)$$

$$Q_4 = \frac{\beta_4 F_f p_f}{2a} - \frac{\pi d_b{}^3 F_{yb}}{32a} - \frac{b_f t_p{}^2}{8a} \sqrt{F_{py}{}^2 - 3(\beta_4 F_f/b_f t_p)^2} \qquad (2.21)$$

$$B_4 = \beta_4 F_f/2 + Q_4 \qquad \text{when } F_1 \le \beta_4\ F_f \le F_{11} \qquad (2.22)$$

$$Q_{4max} = \frac{w' tp^2}{4a} \sqrt{F_{py}{}^2 - 3(F'/w' t_p)^2} \qquad (2.23)$$

$$F' = \text{minimum} \left| \begin{array}{l} F_{limit} = F_{11}/2 \\ F_{4max} = \beta_4 F_f/2 \end{array} \right. \qquad (2.24)$$

$$B_4 = \beta_4 F_f/2 + Q_{4max} \qquad \text{when } \beta_4 F_f > F_{11} \qquad (2.25)$$

The reader is cautioned that the quantities under the radicals in Equations 2.14, 2.16, 2.21, and 2.23 can be

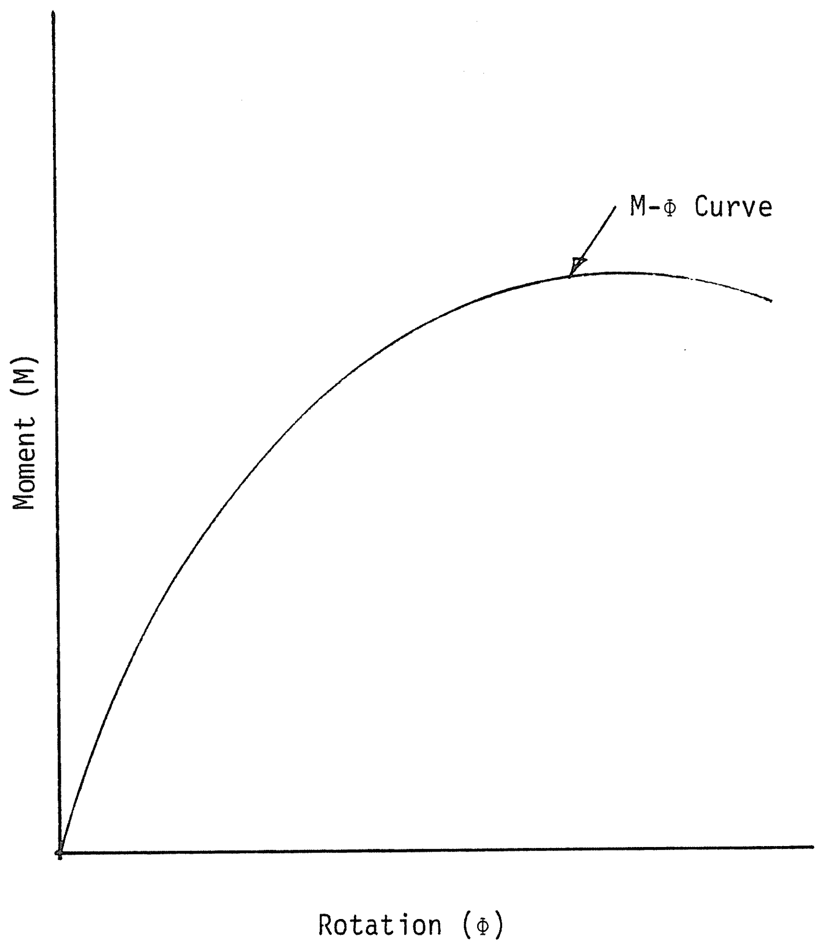

Figure 2.6 Typical M-Φ Diagram

For beams, guidelines have been suggested [7,8] to correlate M-Φ connection behavior and AISC Construction Type. A Type I connection should carry an end moment greater than or equal to 90% of the full fixity end moment and not rotate more than 10% of the simple span rotation. A Type II connection should resist an end moment less than or equal to 20% of the full fixity end moment and rotate at least 80% of the simple span beam end rotation. A Type III connection lies between the limits of the Type I and Type II connections.

The simple span beam end rotation for any loading is given by:

$$\Theta_S = M_F L/2EI \tag{2.26}$$

Then, assuming M_F is the yield moment of the beam, SF_Y, and with I/S = h/2:

$$\Theta_S = F_Y L/Eh \tag{2.27}$$

Taking as a limit L/h equal to 24, and with F_Y equal to 50 ksi and E equal to 29,000 ksi:

$$0.1\Theta_S = 0.00414 \text{ radians} \tag{2.28}$$

This value is used in Section 4.3 to determine the suitability of the tested connections for Type I Construction.

CHAPTER III

EXPERIMENTAL INVESTIGATION

3.1 Test Setup and Procedure

A series of six tests were performed to verify the yield-line theory and modified Kennedy method predictions for the multiple row extended 1/3 moment end-plate connection. The test specimens consisted of end-plates welded to two beam sections which were in turn bolted together in the beam-to-beam connection configuration shown in Figure 3.1. Load was applied to the test specimen by a hydraulic ram via a load cell, swivel head, and spreader beam, as shown in Figure 3.2. The end-plates were subjected to pure moment as the test beam was simply supported and loaded with two equal concentrated loads symmetrically placed. Lateral support for both the test specimen and the spreader beam was provided by lateral brace mechanisms bolted to three steel wide flange frames anchored to the reaction floor of the laboratory.

Each test setup was instrumented with a load cell, three displacement transducers, a gaged caliper, a clip gage, four instrumented bolts, and twenty-six strain gages. Data was collected, processed, and recorded with an HP 3497A Data Acquisition/Control Unit and an HP 85 Computer. Real time plots of selected data were made with an HP 7470A Plotter permitting effective monitoring of the test.

The load cell measured the load applied by the

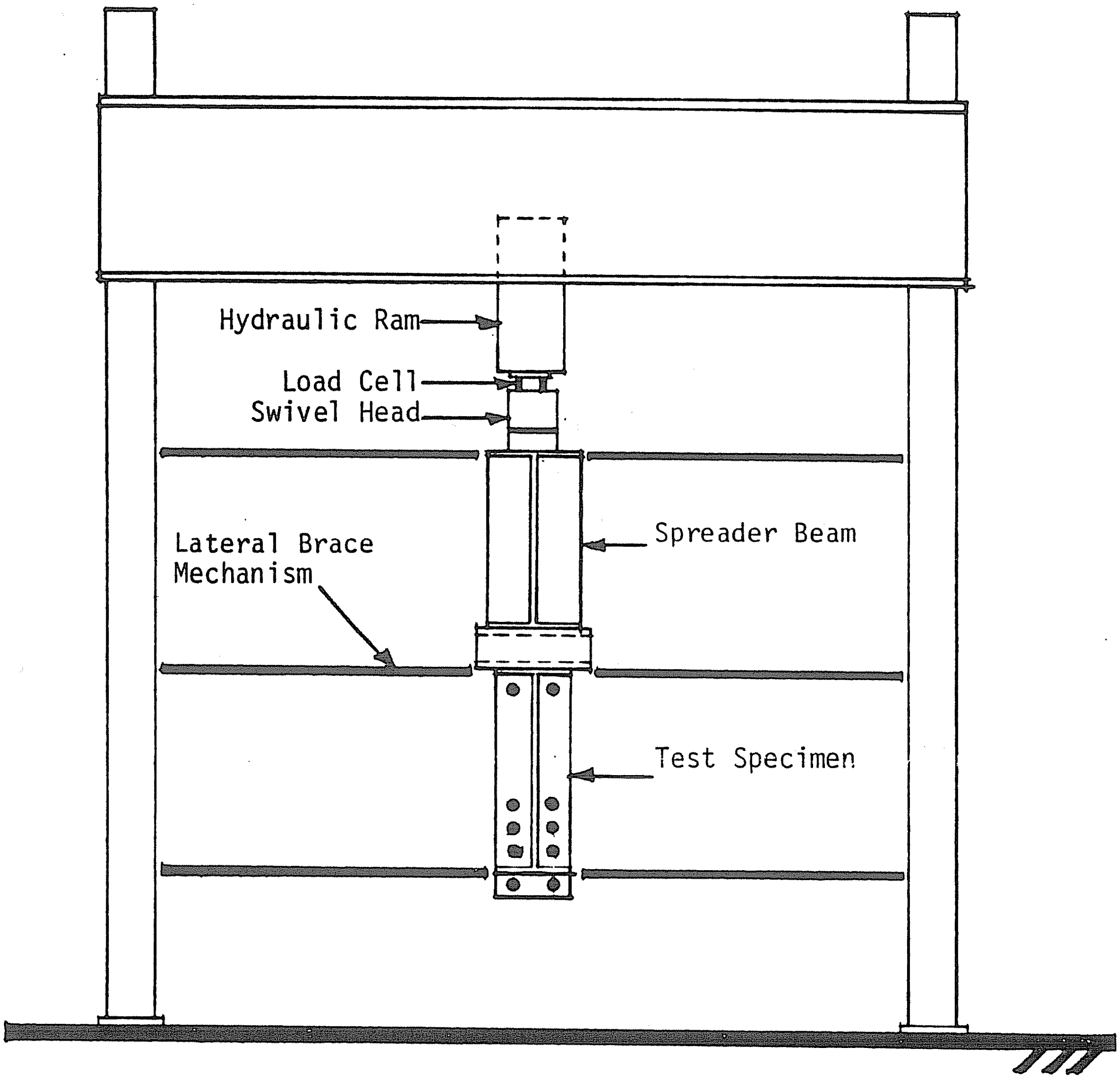

Figure 3.2 Test Setup Transverse Section

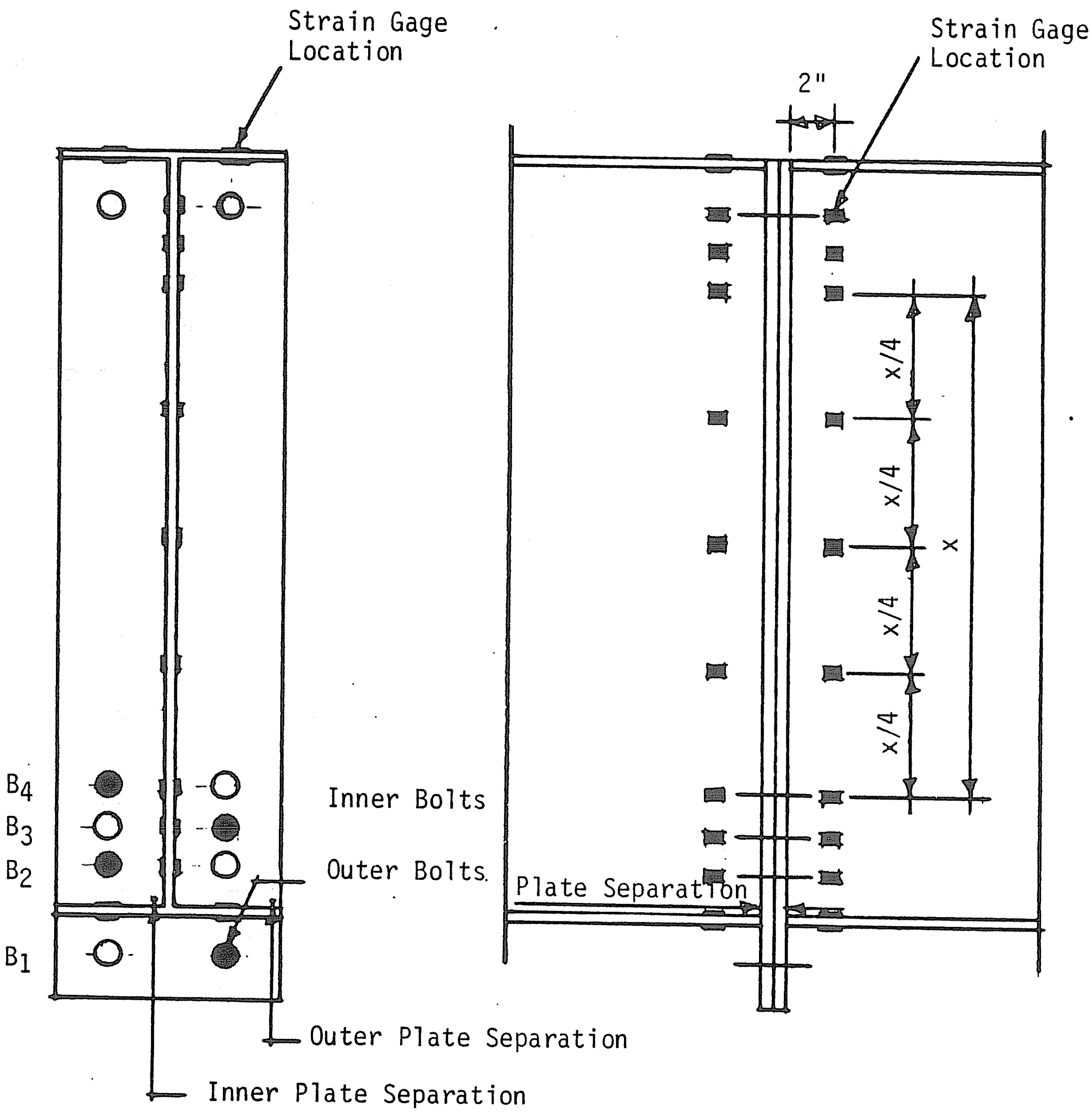

Note: Gaged bolts shown shaded

Figure 3.3 Location of Test Specimen Instrumentation

Table 3.1 Multiple Row Extended 1/3 Moment End-Plate Parameters

Test Designation	t_p (in)	d_b (in)	p_{ext} (in)	p_f (in)	p_b (in)	g (in)	h (in)	b_f (in)	t_w (in)	t_f (in)	F_{py} (ksi)	b (ft)	L (ft)
MRE1/3-3/4-3/8-30	0.377	0.750	2.688	1.105	2.280	2.720	29.813	8.000	0.243	0.377	52.3	13.974	40.031
MRE1/3-1-1/2-30	0.501	1.000	3.404	1.567	3.019	4.574	30.003	8.063	0.260	0.377	50.1	13.935	40.000
MRE1/3-7/8-7/16-46	0.445	0.875	2.894	1.435	2.391	3.253	45.994	8.112	0.353	0.495	62.1	15.987	44.089
MRE1/3-1 1/8-5/8-46	0.634	1.125	3.815	1.742	3.020	3.949	46.026	8.241	0.386	0.498	57.2	15.966	44.089
MRE1/3-1 1/4-5/8-62	0.626	1.250	4.225	2.403	3.505	4.482	62.080	9.941	0.375	1.004	53.9	16.906	45.099
MRE1/3-1 1/2-3/4-62	0.753	1.500	5.130	2.584	4.516	5.559	61.945	9.926	0.375	1.005	54.6	16.924	44.917

The second plot is end-plate separation versus applied moment. Both the inner and outer end-plate separation curves from the experimental test results are presented. The predicted ultimate moment from a yield-line analysis of the end-plate is also shown on this plot.

The third sheet contains two plots. Each plot is moment versus bolt force. The first plot contains two curves for the outer bolt force B_1: the modified Kennedy method prediction and the experimental test results. The second plot similarly contains two curves for the inner bolt force B_2: the modified Kennedy method prediction and the experimental test results. The predicted curves are plotted only for values less than or equal to the bolt proof load. Note that the "bolt force" plotted is a measured change in voltage divided by a calibration factor for a bolt. Since an instrumented bolt is calibrated only in the elastic range, measured "bolt force" is likewise only valid in the elastic range which is less than or equal to the bolt proof load. Actually, the plots represent the change in strain in the bolt shank.

The fourth sheet also contains two plots of moment versus bolt force. The first plot contains two curves for the inner bolt force B_3: the modified Kennedy method prediction and the experimental test results. The second plot similarly contains two curves for the inner bolt force B_4: the modified Kennedy method prediction and the experimental test results. The predicted curves are plotted only for values less than or equal to the bolt proof load.

The fifth and final sheet contains a single plot of moment versus rotation or M-Φ diagram. The M-Φ curve is developed by solving the following for the connection rotation, Φ:

Table 3.2

Tensile Coupon Test Results

Coupon	Yield Stress (ksi)	Tensile Stress (ksi)	Elongation (%)
MRE1/3-3/4-3/8-30	52.3	79.4	59.4
MRE1/3-1-1/2-30	50.1	79.0	62.5
MRE1/3-7/8-7/16-46	62.1	79.2	53.1
MRE1/3-1 1/8-5/8-46	57.2	80.0	65.6
MRE1/3-1 1/4-5/8-62	53.9	75.8	67.2
MRE1/3-1 1/2-3/4-62	54.6	76.0	75.0

CHAPTER IV

COMPARISON OF EXPERIMENTAL TEST RESULTS AND PREDICTIONS

4.1 End-Plate Strength Comparisons

The ultimate moment capacity for each experimental test specimen was calculated using Equation 2.3 or 2.5 as appropriate and the measured yield stress in Table 3.2. The maximum applied moment, predicted ultimate moment, and the ratio of predicted-to-applied moment for each experimental test are shown in Table 4.1. The predicted-to-applied moment ratios varied from 0.61 (more conservative) to 0.99 (less conservative). From the moment versus plate separation plots in the appendices, the predicted ultimate moment corresponds very closely to the yield plateau of each plate separation curve.

Two of the experimental tests, MRE1/3-1-1/2-30 and MRE1/3-7/8-7/16-46, were terminated at lower load levels than desired. Nonetheless, the behavior of these two tests closely corresponds to that observed for the remaining four experimental tests as shown by the moment versus plate separation curves.

4.2 Bolt Force Comparisons

Table 4.1 lists the applied and predicted moments at which bolt proof load was reached in the outer and inner bolts for each experimental test. The bolt proof load is twice the allowable AISC Specification tension capacity. For A325 bolts, the proof load is calculated with 88 ksi and the bolt area based on nominal bolt diameter. Proof loads are 38.9 kips for 3/4 inch diameter bolts, 52.9 kips for 7/8 inch diameter bolts, 69.1 kips for 1 inch diameter bolts, 87.5 kips for 1-1/8 inch diameter bolts, 108.0 kips for 1-1/4 inch diameter bolts, and 155.5 kips for 1-1/2 inch diameter bolts. These valves are shown on the moment versus bolt force plots in the appendices.

The predicted moments are obtained by determining values for the factors α in Equation 2.9; β_2 in Equations 2.13, 2.15, and 2.19; β_3 in Equation 2.10; and β_4 in Equations 2.20, 2.22, and 2.25. These factors proportion the beam tension flange force to the outer and inner end-plates. Factors α, β_2, β_3, and β_4 were empirically determined from the experimental test data as:

$$\alpha = 0.60 \tag{4.1}$$

$$\beta_2 = 0.35 \tag{4.2}$$

$$\beta_3 = 0.45 \tag{4.3}$$

$$\beta_4 = 0.25 \tag{4.4}$$

Hence, $\alpha + \beta_2 + \beta_3 + \beta_4 = 1.65$.

In three of the four experimental tests for which comparative results are available, the inner bolt B_2 reached bolt proof load before outer bolt B_1. Considering the applied moments at which the inner bolt B_2 reached proof load, a $\beta_2 = 0.35$ was selected to best represent the experimental test data. The predicted-to-applied moment ratios for the inner bolt B_2 at proof load with $\beta_2 = 0.35$, range from 0.76 to 1.15. The experimental data show that the inner bolt B_2 force, actually a strain, increased at an increasing rate after the bolt proof load was reached. This indicates that the inner bolt B_2 was not accepting significant additional beam tension flange force.

CHAPTER V

DESIGN RECOMMENDATIONS AND EXAMPLE

5.1 Design Recommendations

This study continues the unification of design procedures for moment end-plate connections established by Hendrick *et al* [2] and extended by Morrison *et al* [3] to include a sixth configuration, the multiple row extended 1/3 moment end-plate connection. This unification provides consistent analytical procedures: end-plate strength criterion by yield-line theory and bolt force prediction by a modified Kennedy method. Further, an assessment of the connection rotational stiffness via M-Φ diagrams is presented. These analytical procedures are verified with adequate experimental testing.

The recommended design procedure follows:

1. Compute the factored beam end moment:

$$M_u = M_w/0.6 \tag{5.1}$$

2. Establish values to define the end-plate geometry:

b_f, g, h, P_t, P_f, P_b, d_e, and t_w.

3. With a known yield stress, F_{py}, determine the required end-plate thickness using the flow chart in Figure 5.1.

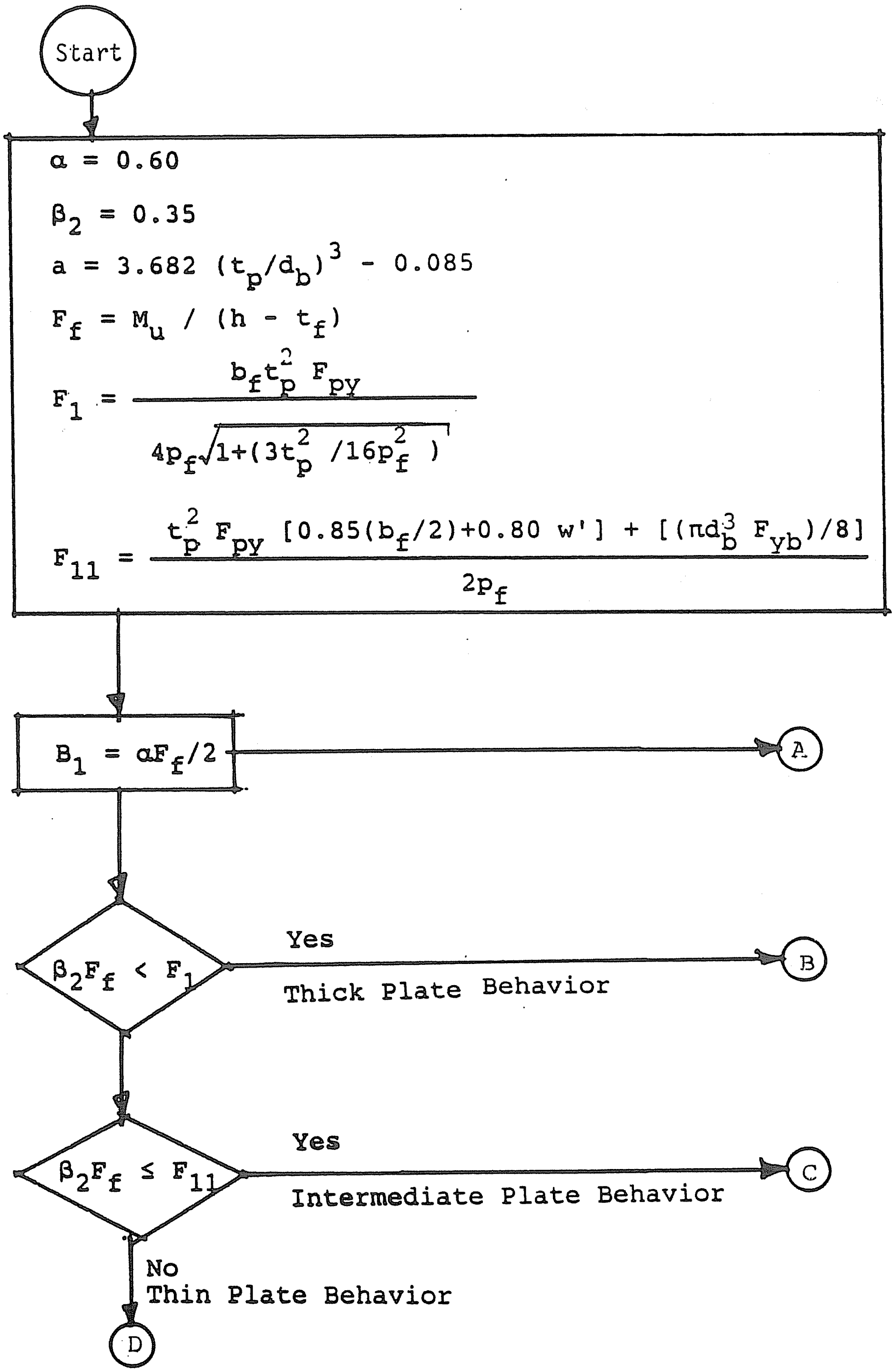

Figure 5.2 Flowchart to Determine Controlling Bolt Force

4. Select a trial bolt diameter and compute the controlling bolt force using the flowchart in Figure 5.2.

5. The required bolt diameter is determined from:

$$d_b = \sqrt{2B_c/(\pi\ F_a)} \tag{5.2}$$

where F_a = the allowable stress for the bolt material.

In the AISC Specification [5], the allowable tensile stress for A325 bolt material is 44 ksi with a factor of safety against yielding of 2.0. Equation 5.2 reflects this factor of safety.

Geometric limitations for the design procedure are found in Table 1.1. This procedure is demonstrated in Section 5.2.

5.2 Design Example

Determine the required end-plate thickness and bolt size for a multiple row extended 1/3 moment end-plate connection given the following:

Beam data...	
A572 Gr 50 material	F_y = 50. ksi
Depth	h = 62 in
Flange width	b_f = 10 in
Web thickness	t_w = 3/8 in
Flange thickness	t_f = 1 in
End-plate data...	
A572 Gr 50 material	F_{py} = 50 ksi
Extension outside beam flange	p_{ext} = 4-1/4 in

$$t_p = \left\{ \frac{M_u/F_{py}}{(b_f/2)[1/2 + h/p_f + (h-p_t)/p_f + (h - p_{t3})/u] + (2/g)(p_f + p_{b1,3} + u)(h - p_t)} \right\}^{\frac{1}{2}}$$

$$= \left\{ \frac{1166.7(12)/50}{(10/2)[1/2 + 62/2.375 + (62 - 2.375)/2.375 + (62 - 10.375)/3.15] + 2/4.5)(2.375 + 7.0 + 3.15)(62 - 3.375)} \right\}^{\frac{1}{2}}$$

$$= 0.649 \text{ in.}$$

<u>Step 3.</u> Determine u and required end-plate thickness for Mechanism 2.

$$u = (1/2)\sqrt{b_f g}$$

$$= (1/2)\sqrt{10(4.5)} = 3.35 \text{ in.}$$

$$t_p = \left\{ \frac{M_u/F_{py}}{(b_f/2)[1/2 + h/p_f + (h - p_t)/p_f + (h - p_{t3})/u] + (2/g)(p_f+p_{b1,3})(h-t_f)+(2u/g)(h-p_{t3})+(g/2)} \right\}^{\frac{1}{2}}$$

Step 7. Determine inner end-plate behavior.

$$F_1 = \frac{b_f t_p^2 F_{py}}{4p_f\sqrt{1+(3t_p^2/16p_f^2)}}$$

$$= \frac{10(0.688)^2(50)}{4(2.375)\sqrt{1+[3(0.688)^2/16(2.375)^2]}} = 24.7 \text{ kips}$$

Try 1 in. diameter bolts.

$$w' = (b_f/2) - [d_b - (1/16)]$$

$$= (10/2) - [1.0 - (1/16)] = 4.06 \text{ in.}$$

$$F_{11} = \frac{t_p^2 F_{py}[0.85(b_f/2) + 0.80\ w'] + [\pi d_b^3 F_{yb})/8]}{2p_f}$$

$$= \frac{(0.688)^2\ 50[0.85(10/2) + 0.80(4.06)] + [\pi(1.0)^3(88)/8]}{2(2.375)}$$

$$= 44.6 \text{ kips}$$

Since $\beta_2 F_f = 0.35(229.5) = 80.3$ kips $> F_{11} = 44.6$ kips, inner end-plate behavior is thin.

Step 8. Determine inner bolt B_2 force.

$$a = 3.682\ (t_p/d_b)^3 - 0.085$$

$$= 3.682\ (0.688/1.0)^3 - 0.085 = 1.114 \text{ in.}$$

Summary. For materials, geometry, and given loading, use A572 Gr 50 end-plate with 11/16 in. thickness and 1 in. diameter A325 bolts.

REFERENCES

1. Srouji, R., Kukreti, A., and Murray, T., "Yield-Line Analysis of End-Plate Connections with Bolt Force Predictions", Fears Structural Engineering Laboratory Report No. FSEL/MBMA 83-05, University of Oklahoma, Norman, Oklahoma, December 1983.

2. Hendrick, D., Kukreti, A., and Murray, T., "Unification of Flush End-Plate Design Procedures", Fears Structural Engineering Laboratory Report No. FSEL/MBMA 85-01, University of Oklahoma, Norman, Oklahoma, March 1985.

3. Morrison, S., Astaneh-Asl, A., and Murray, T., "Analytical and Experimental Investigation of the Extended Stiffened Moment End-Plate Connection with Four Bolts at the Beam Tension Flange", Fears Structural Engineering Laboratory Report No. FSEL/MBMA 85-04, University of Oklahoma, Norman, Oklahoma, December 1985.

4. Kennedy, N.A., Vinnakota, S., and Sherbourne, A.N., "The Split-Tee Analogy in Bolted Splices and Beam-Column Connections", Joints in Structural Steelwork, Proceedings of the International Conference on Joints in Steelwork, held at Middlesbrough, Cleveland, John Wiley and Sons, New York - Toronto, 1981, pp. 2.138-2.157.

5. "Specification for the Design, Fabrication and Erection of Structural Steel for Buildings", American Institute of Steel Construction, New York, 1978.

6. Manual of Steel Construction, 8th ed., American Institute of Steel Construction, Chicago, Illinois, 1980.

7. Salmon, C.G. and Johnson, V.E., Steel Structures Design and Behavior, 2nd ed., Harper and Row, New York, 1980, pp. 729-733.

8. McGuire, W., Steel Structures, Prentice-Hall, Englewood Cliffs, New Jersey, 1968, pp. 890-914.

APPENDIX A

NOMENCLATURE

NOMENCLATURE

a = distance from bolt centerline to prying force for plate

B = bolt force

B_1 = outer bolt force

B_2 = inner bolt force; first bolt from beam tension flange

B_3 = inner bolt force; second bolt from beam tension flange

B_4 = inner bolt force; third bolt from beam tension flange

b = distance from concentrated load to support for test specimen

b_f = beam flange width

d_b = bolt diameter

d_e = distance from bolt centerline to edge of end-plate extension

E = Young's modulus of elasticity

F = force

F_a = bolt material allowable stress

F_f = flange force
 $= M_u / (h - t_f)$

F_{limit} = possible flange force per bolt at the thin plate limit

F_{max} = possible flange force per bolt at the thin plate limit

F_{py} = plate material yield stress

F_y = yield stress

p_t = distance from bolt centerline B_2 to far face of beam flange

= $p_f + t_f$

p_{t2} = distance from bolt centerline B_3 to far face of beam flange

= $p_t + p_b$

p_{t3} = distance from bolt centerline B_4 to far face of beam flange

= $p_t + 2p_b$

Q = prying force

Q_{max} = maximum prying force

Q_2 = prying force for bolt B_2

Q_{2max} = maximum prying force for bolt B_2

Q_4 = prying force for bolt B_4

Q_{4max} = maximum prying force for bolt B_4

S = section modulus

t_f = beam flange thickness

t_p = end-plate thickness

t_w = beam web thickness; stiffener thickness

t_1 = plate thickness at thick plate limit

t_{11} = plate thickness at thin plate limit

u = distance from bolt centerline B_4 to outermost yield-line

w = end-plate width per bolt pair

w' = end-plate width per bolt less bolt hole diameter (at bolt line)

x = distance

α = outer end-plate factor

β_2 = inner end-plate factor for bolt B_2

β_3 = inner end-plate factor for bolt B_3

β_4 = inner end-plate factor for bolt B_3

δ_{pred} = predicted strength of materials centerline deflection for test specimen

δ_{test} = experimental test centerline deflection for test specimen

Θ_s = simple span end rotation for any loading

π = pi

Φ = rotation

APPENDIX B

MRE1/3-3/4-3/8-30 TEST RESULTS

TEST SYNOPSIS

PROJECT:	MBMA END-PLATE
TEST:	MRE1/3-3/4-3/8-30
TEST DATE:	10-2-85
CONNECTION DESCRIPTION:	Multiple row extended 1/3 moment end-plate with a single row of two bolts outside and three rows of two bolts inside the beam tension flange

BEAM DATA:				
Depth	h	(in)	=	29.813
Flange width	bf	(in)	=	8.000
Web thickness	tw	(in)	=	0.243
Flange thickness	tf	(in)	=	0.377
Moment of inertia	I	(in**4)	=	1876.2
END-PLATE:				
Thickness	tp	(in)	=	0.377
Extension outside beam flange	pext	(in)	=	2.688
Pitch to bolt from flange	pf	(in)	=	1.105
Pitch between bolt rows	pb	(in)	=	2.280
Gage	g	(in)	=	2.720
Steel yield stress	Fpy	(in)	=	52.3
BOLT DATA:				
Type			=	A325
Diameter	db	(in)	=	0.750
Pretension force	Tb	(k)	=	28.0
PREDICTION:				
End-plate failure moment	Mu	(k-ft)	=	325.6
Bolt failure (proof) moment	Myb	(k-ft)	=	318.1
Beam failure moment		(k-ft)	=	527.8
EXPERIMENTAL:				
Maximum applied moment		(k-ft)	=	404.9
Moment at bolt proof load		(k-ft)	=	297.5
Maximum vertical centerline deflection		(in)	=	3.214
Maximum inner end-plate separation		(in)	=	0.0867
Maximum outer end-plate separation		(in)	=	0.0321

DISCUSSION:

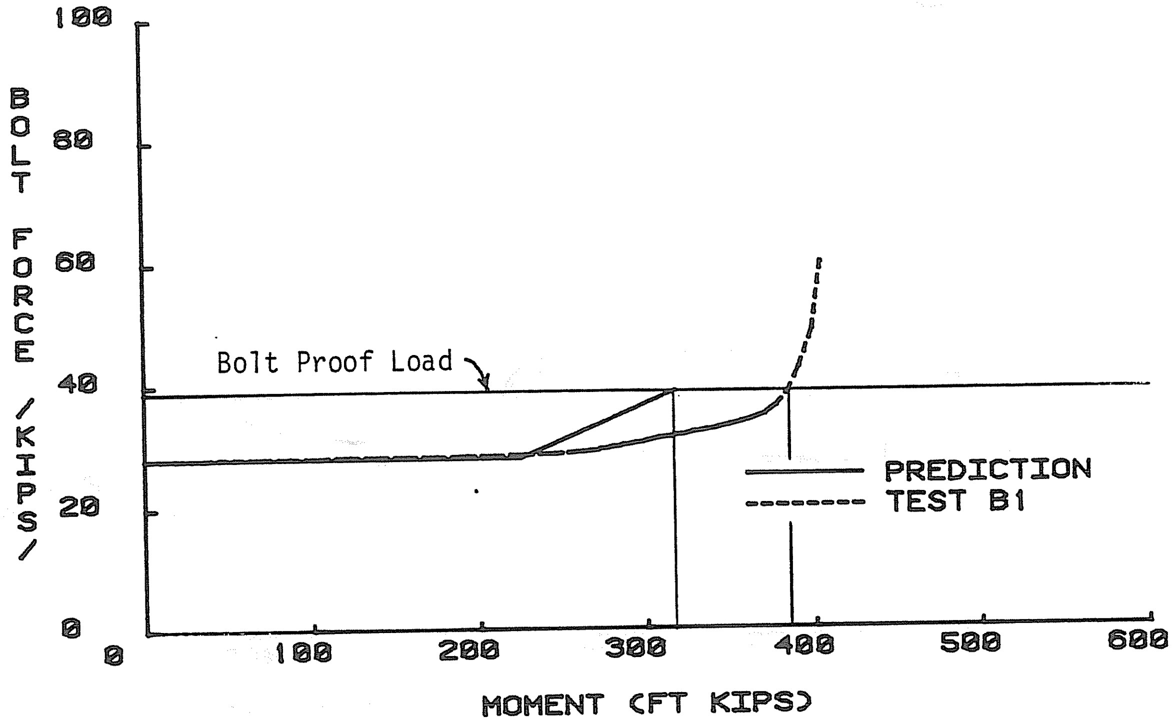

(c) Outer Bolt Force B_1 versus End-Plate Moment

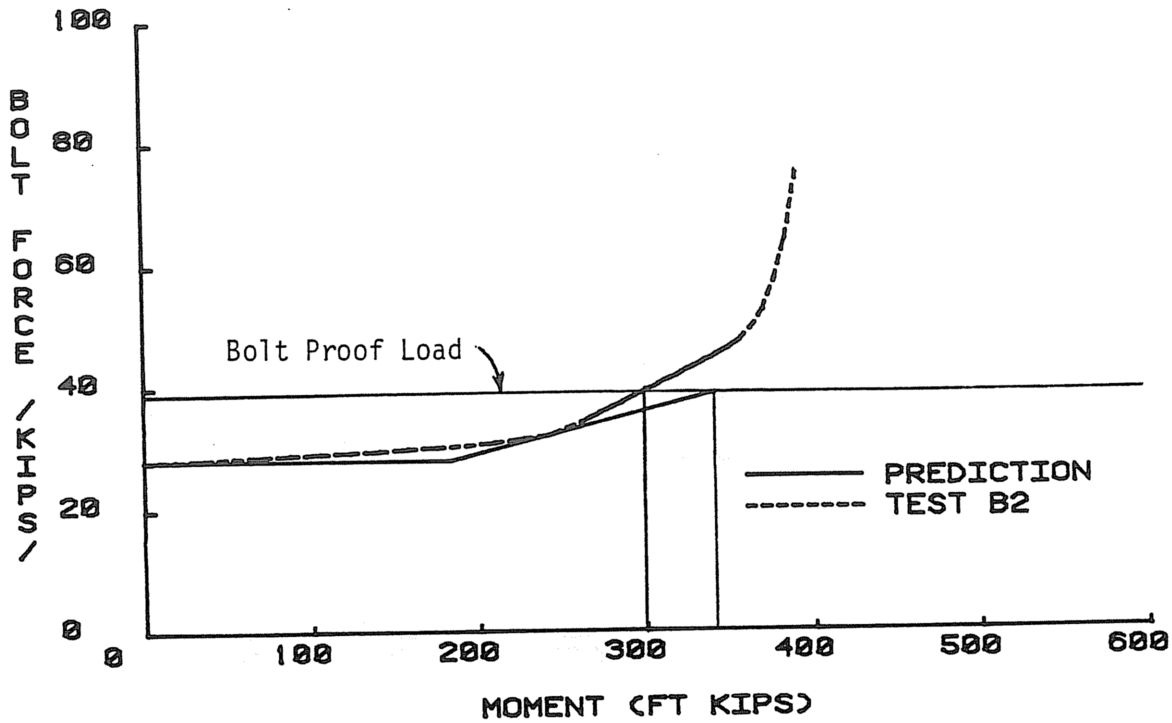

(d) Inner Bolt Force B_2 versus End-Plate Moment

Figure B.1 Results from Test MRE1/3-3/4-3/8-30, Continued

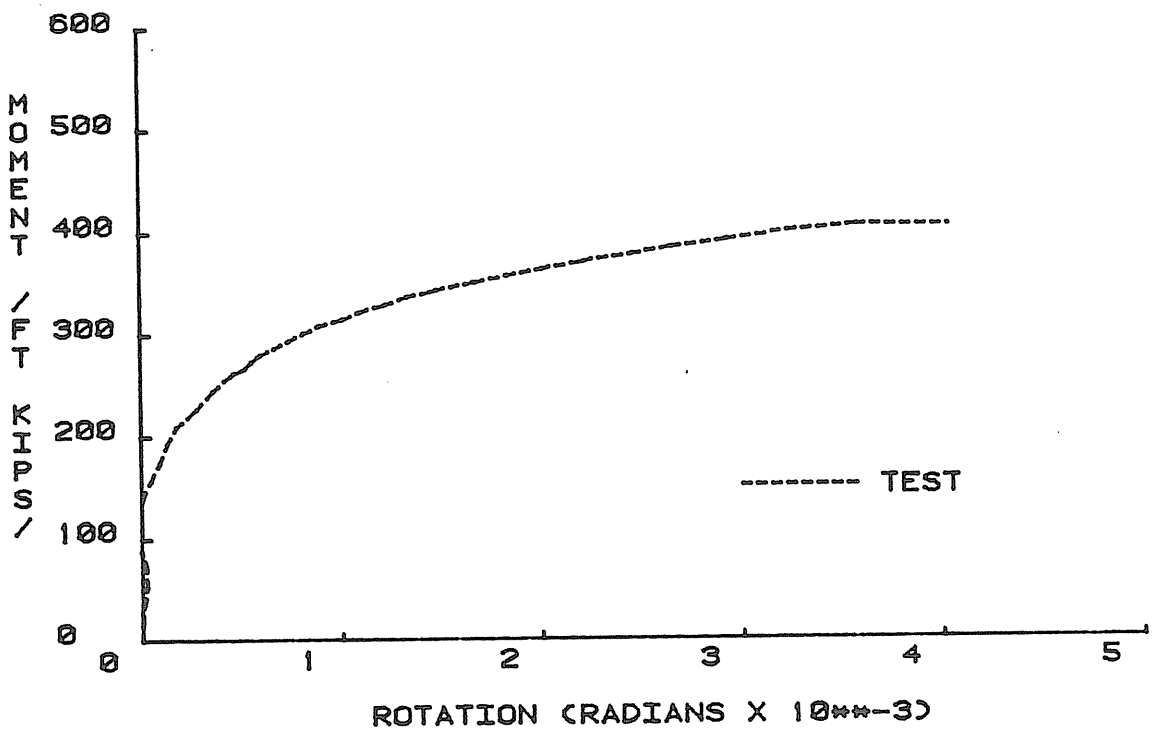

(g) End-Plate Moment versus Rotation

Figure B.1 Results from Test MRE1/3-3/4-3/8-30, Continued

APPENDIX C

MRE1/3-1-1/2-30 TEST RESULTS

TEST SYNOPSIS

PROJECT:	MBMA END-PLATE
TEST:	MRE1/3-1-1/2-30
TEST DATE:	10-25-85
CONNECTION DESCRIPTION:	Multiple row extended 1/3 moment end-plate with a single row of two bolts outside and three rows of two bolts inside the beam tension flange

BEAM DATA:				
Depth	h	(in)	=	30.003
Flange width	bf	(in)	=	8.063
Web thickness	tw	(in)	=	0.260
Flange thickness	tf	(in)	=	0.377
Moment of inertia	I	(in**4)	=	1876.2
END-PLATE:				
Thickness	tp	(in)	=	0.501
Extension outside beam flange	pext	(in)	=	3.404
Pitch to bolt from flange	pf	(in)	=	1.567
Pitch between bolt rows	pb	(in)	=	3.019
Gage	g	(in)	=	4.574
Steel yield stress	Fpy	(in)	=	50.1
BOLT DATA:				
Type			=	A325
Diameter	db	(in)	=	1.000
Pretension force	Tb	(k)	=	51.0
PREDICTION:				
End-plate failure moment	Mu	(k-ft)	=	258.9
Bolt failure (proof) moment	Myb	(k-ft)	=	570.0
Beam failure moment		(k-ft)	=	523.2
EXPERIMENTAL:				
Maximum applied moment		(k-ft)	=	425.1
Moment at bolt proof load		(k-ft)	=	------
Maximum vertical centerline deflection		(in)	=	3.445
Maximum inner end-plate separation		(in)	=	0.0383
Maximum outer end-plate separation		(in)	=	0.0694

DISCUSSION:

A hydraulic problem occurred during the final test setup loading sequence. The test was terminated at lower load levels than anticipated.

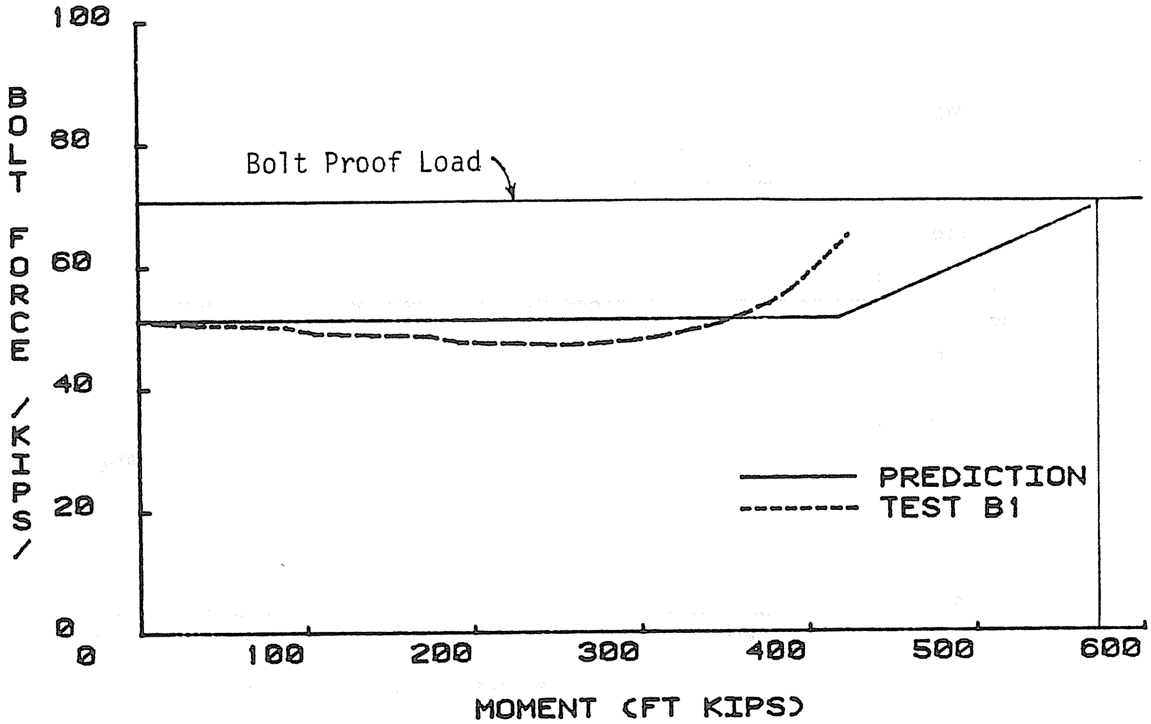

(c) Outer Bolt Force B_1 versus End-Plate Moment

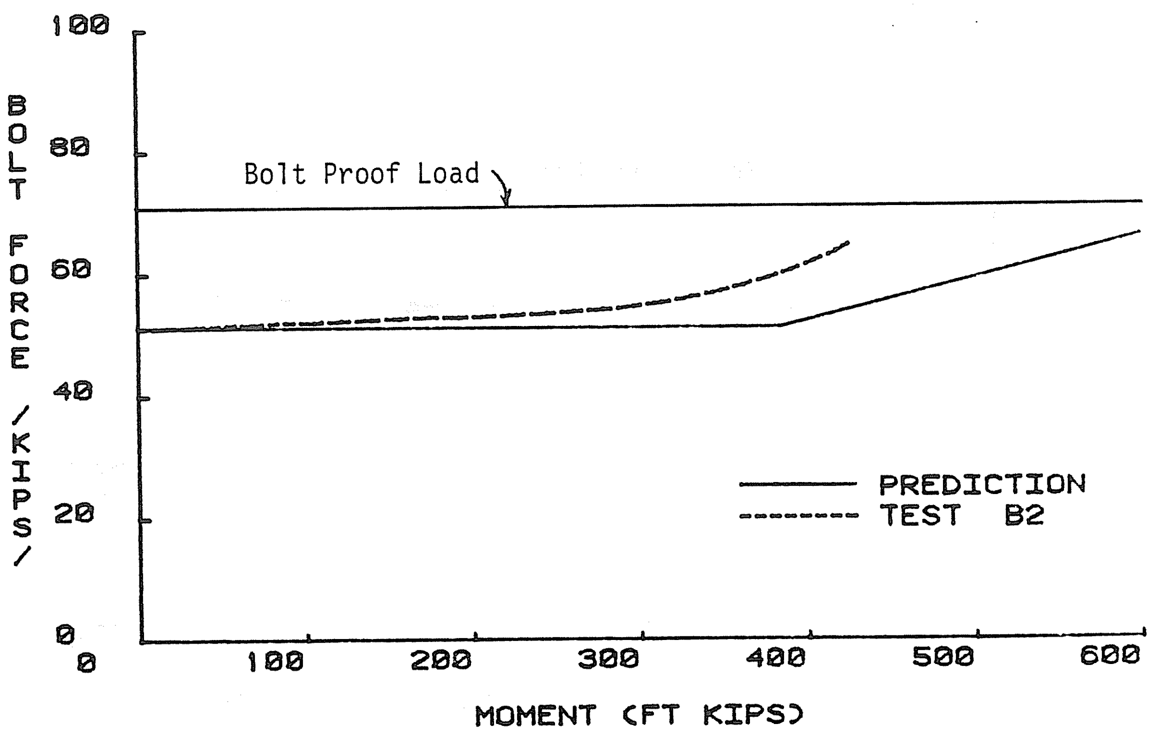

(d) Inner Bolt Force B_2 versus End-Plate Moment

Figure C.1 Results from Test MRE1/3-1-1/2-30, Continued

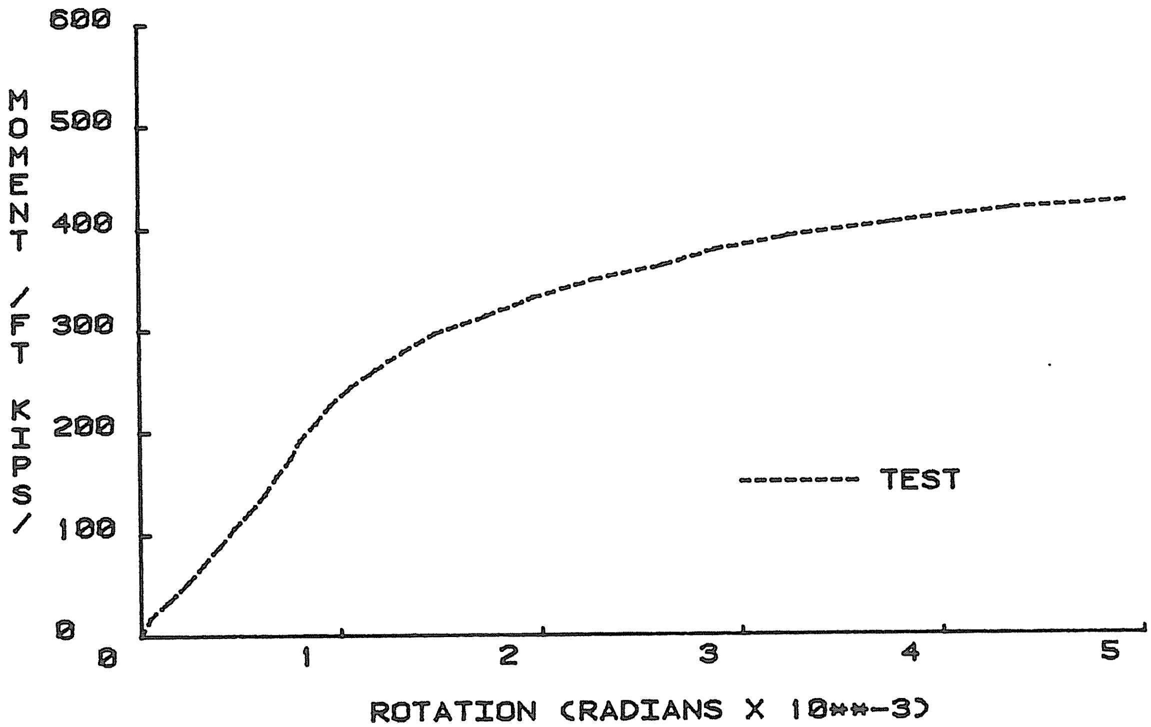

(g) End-Plate Moment versus Rotation

Figure C.1 Results from Test MRE1/3-1-1/2-30, Continued

APPENDIX D

MRE1/3-7/8-7/16-46 TEST RESULTS

TEST SYNOPSIS

PROJECT:	MBMA END-PLATE			
TEST:	MRE1/3-7/8-7/16-46			
TEST DATE:	11-1-85			
CONNECTION DESCRIPTION:	Multiple row extended 1/3 moment end-plate with a single row of two bolts outside and three rows of two bolts inside the beam tension flange			
BEAM DATA:				
Depth	h	(in)	=	45.994
Flange width	bf	(in)	=	8.112
Web thickness	tw	(in)	=	0.353
Flange thickness	tf	(in)	=	0.495
Moment of inertia	I	(in**4)	=	6834.0
END-PLATE:				
Thickness	tp	(in)	=	0.445
Extension outside beam flange	pext	(in)	=	2.894
Pitch to bolt from flange	pf	(in)	=	1.435
Pitch between bolt rows	pb	(in)	=	2.391
Gage	g	(in)	=	3.253
Steel yield stress	Fpy	(in)	=	62.1
BOLT DATA:				
Type			=	A325
Diameter	db	(in)	=	0.875
Pretension force	Tb	(k)	=	39.0
PREDICTION:				
End-plate failure moment	Mu	(k-ft)	=	570.0
Bolt failure (proof) moment	Myb	(k-ft)	=	643.5
Beam failure moment		(k-ft)	=	1540.9
EXPERIMENTAL:				
Maximum applied moment		(k-ft)	=	866.1
Moment at bolt proof load		(k-ft)	=	838.8
Maximum vertical centerline deflection		(in)	=	1.802
Maximum inner end-plate separation		(in)	=	0.0345
Maximum outer end-plate separation		(in)	=	0.0540

DISCUSSION:

A local buckle occurred adjacent the end-plate in the beam compression flange. The test was terminated at lower load levels than anticipated.

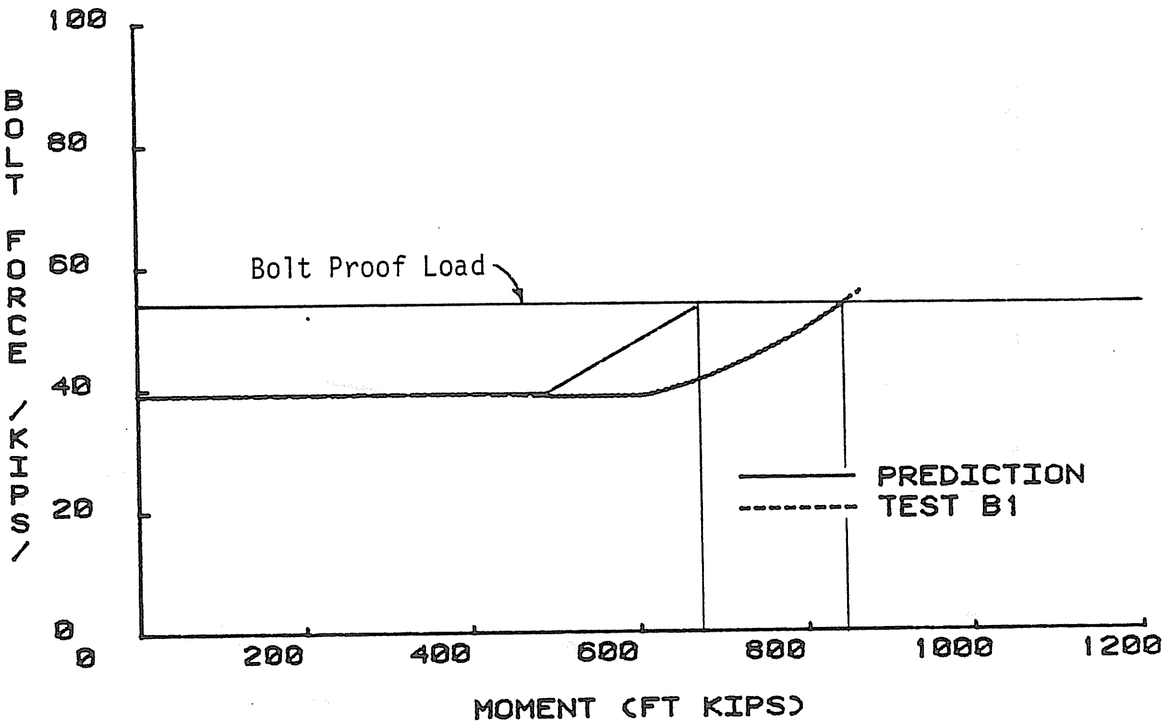

(c) Outer Bolt Force B_1 versus End-Plate Moment

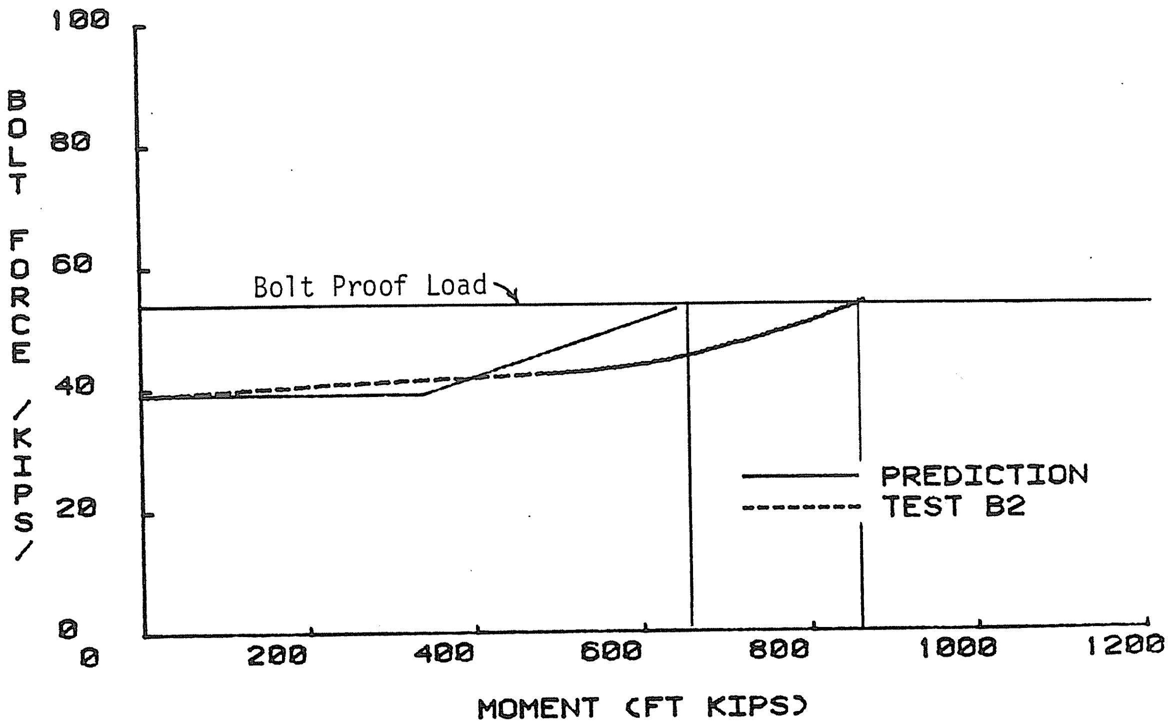

(d) Inner Bolt Force B_2 versus End-Plate Moment

Figure D.1 Results from Test MRE1/3-7/8-7/16-46, Continued

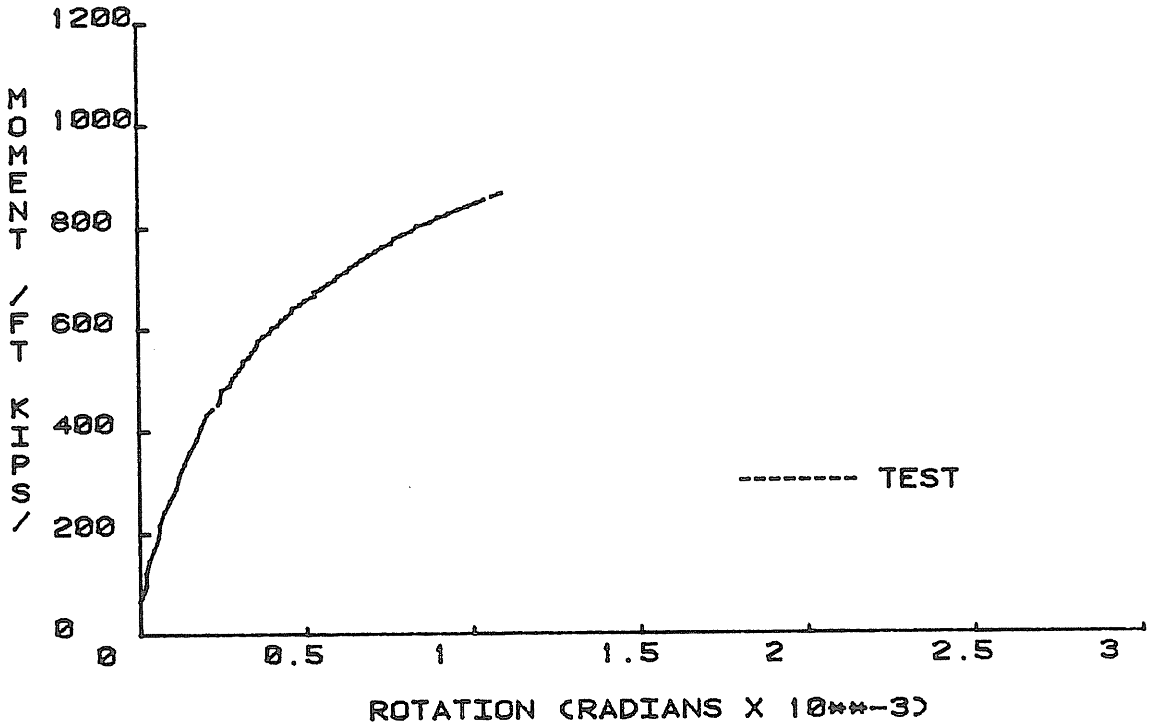

(g) End-Plate Moment versus Rotation

Figure D.1 Results from Test MRE1/3-7/8-7/16-46, Continued

APPENDIX E

MRE1/3-1 1/8-5/8-46 TEST RESULTS

TEST SYNOPSIS

PROJECT:	MBMA END-PLATE
TEST:	MRE1/3-1 1/8-5/8-46
TEST DATE:	11-12-85
CONNECTION DESCRIPTION:	Multiple row extended 1/3 moment end-plate with a single row of two bolts outside and three rows of two bolts inside the beam tension flange

BEAM DATA:				
Depth	h	(in)	=	46.026
Flange width	bf	(in)	=	8.241
Web thickness	tw	(in)	=	0.386
Flange thickness	tf	(in)	=	0.498
Moment of inertia	I	(in**4)	=	7186.8
END-PLATE:				
Thickness	tp	(in)	=	0.634
Extension outside beam flange	pext	(in)	=	3.815
Pitch to bolt from flange	pf	(in)	=	1.742
Pitch between bolt rows	pb	(in)	=	3.020
Gage	g	(in)	=	3.949
Steel yield stress	Fpy	(in)	=	57.2
BOLT DATA:				
Type			=	A325
Diameter	db	(in)	=	1.125
Pretension force	Tb	(k)	=	56.0
PREDICTION:				
End-plate failure moment	Mu	(k-ft)	=	966.7
Bolt failure (proof) moment	Myb	(k-ft)	=	1106.6
Beam failure moment		(k-ft)	=	1491.6
EXPERIMENTAL:				
Maximum applied moment		(k-ft)	=	975.1
Moment at bolt proof load		(k-ft)	=	------
Maximum vertical centerline deflection		(in)	=	1.940
Maximum inner end-plate separation		(in)	=	0.0082
Maximum outer end-plate separation		(in)	=	0.0153

DISCUSSION:

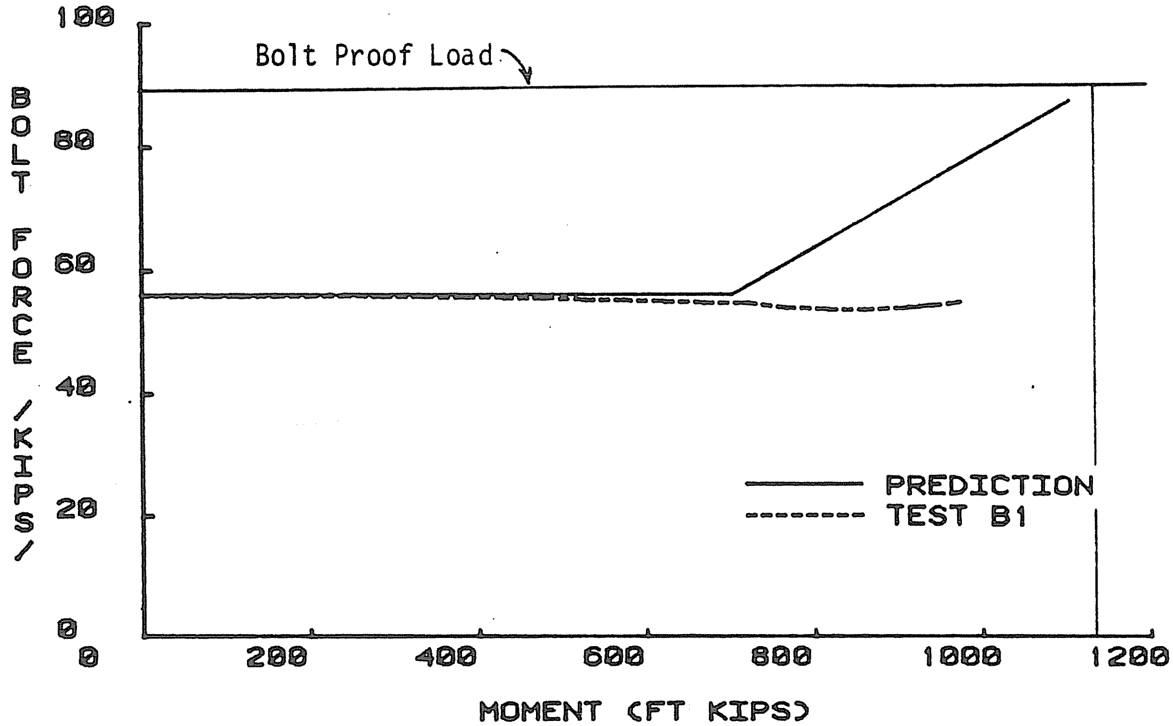

(c) Outer Bolt Force B_1 versus End-Plate Moment

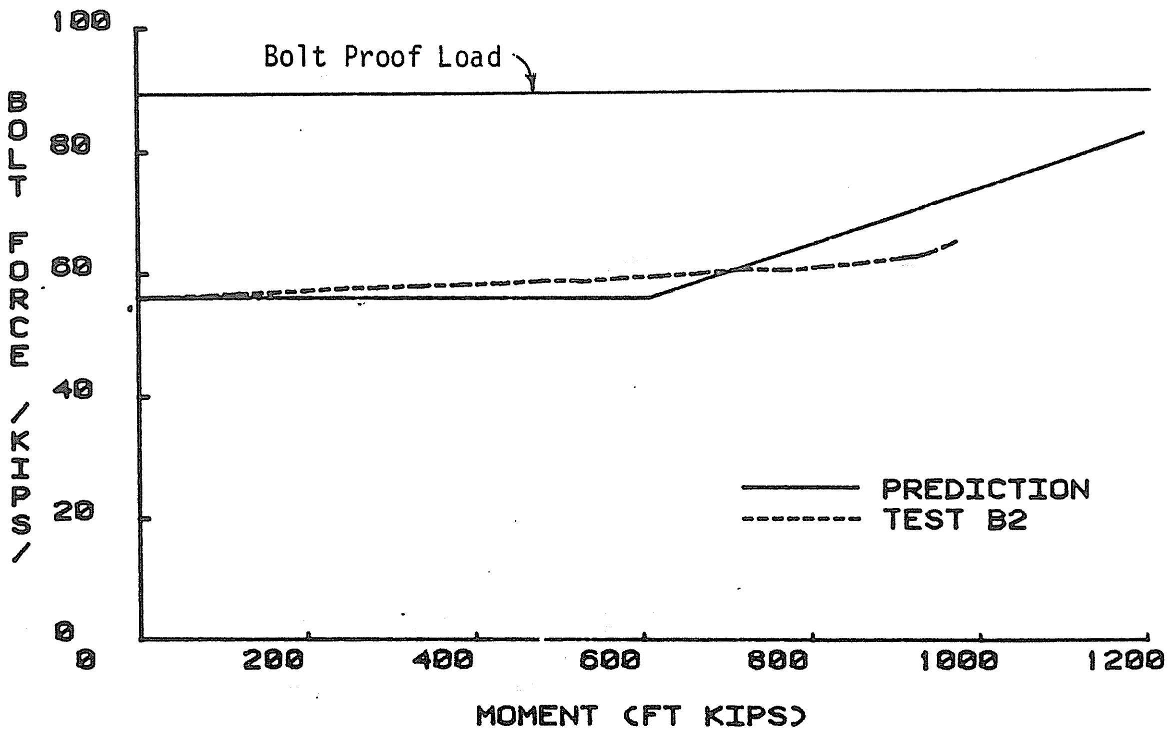

(d) Inner Bolt Force B_2 versus End-Plate Moment

Figure E.1 Results from Test MRE1/3-1 1/8-5/8-46, Continued

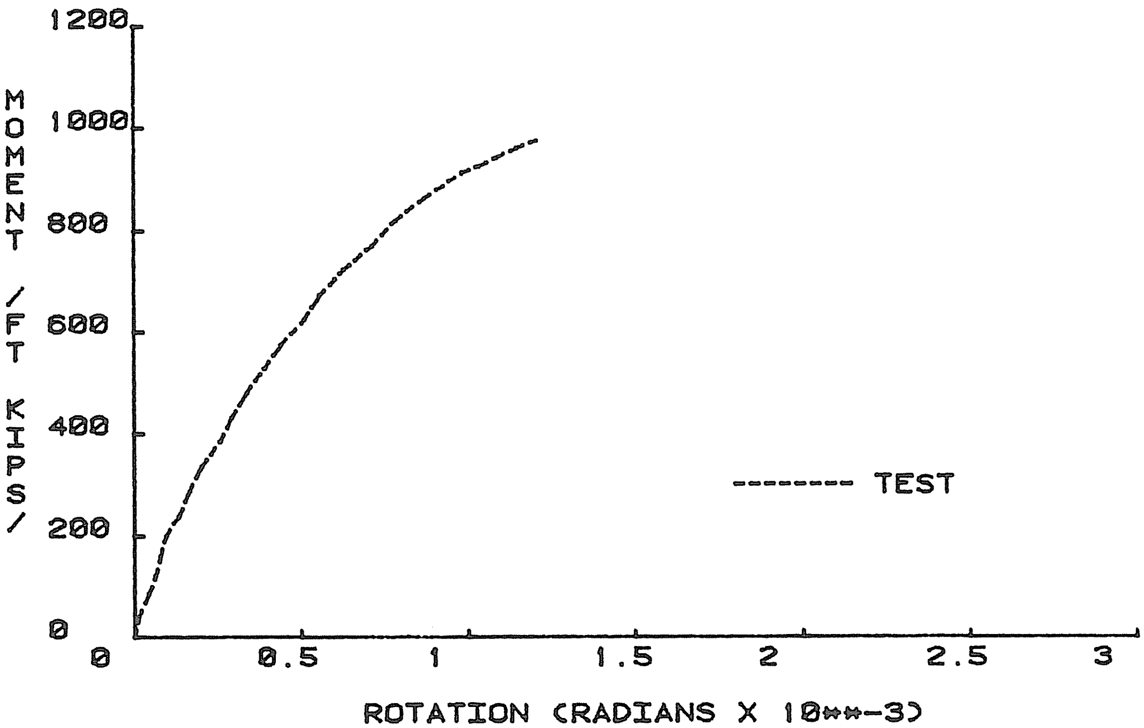

(f) End-Plate Moment versus Rotation

Figure E.1 Results from Test MRE1/3-1 1/8-5/8-46, Continued

APPENDIX F

MRE1/3-1 1/4-5/8-62 TEST RESULTS

TEST SYNOPSIS

PROJECT:	MBMA END-PLATE
TEST:	MRE1/3-1 1/4-5/8-62
TEST DATE:	12-6-85
CONNECTION DESCRIPTION:	Multiple row extended 1/3 moment end-plate with a single row of two bolts outside and three rows of two bolts inside the beam tension flange

BEAM DATA:				
Depth	h	(in)	=	62.080
Flange width	bf	(in)	=	9.941
Web thickness	tw	(in)	=	0.375
Flange thickness	tf	(in)	=	1.004
Moment of inertia	I	(in**4)	=	25,391.5
END-PLATE:				
Thickness	tp	(in)	=	0.626
Extension outside beam flange	pext	(in)	=	4.225
Pitch to bolt from flange	pf	(in)	=	2.403
Pitch between bolt rows	pb	(in)	=	3.505
Gage	g	(in)	=	4.482
Steel yield stress	Fpy	(in)	=	53.9
BOLT DATA:				
Type			=	A325
Diameter	db	(in)	=	1.250
Pretension force	Tb	(k)	=	71.0
PREDICTION:				
End-plate failure moment	Mu	(k-ft)	=	1166.5
Bolt failure (proof) moment	Myb	(k-ft)	=	1690.6
Beam failure moment		(k-ft)	=	3681.6
EXPERIMENTAL:				
Maximum applied moment		(k-ft)	=	1635.0
Moment at bolt proof load		(k-ft)	=	1610.1
Maximum vertical centerline deflection		(in)	=	1.029
Maximum inner end-plate separation		(in)	=	0.0300
Maximum outer end-plate separation		(in)	=	0.572

DISCUSSION:

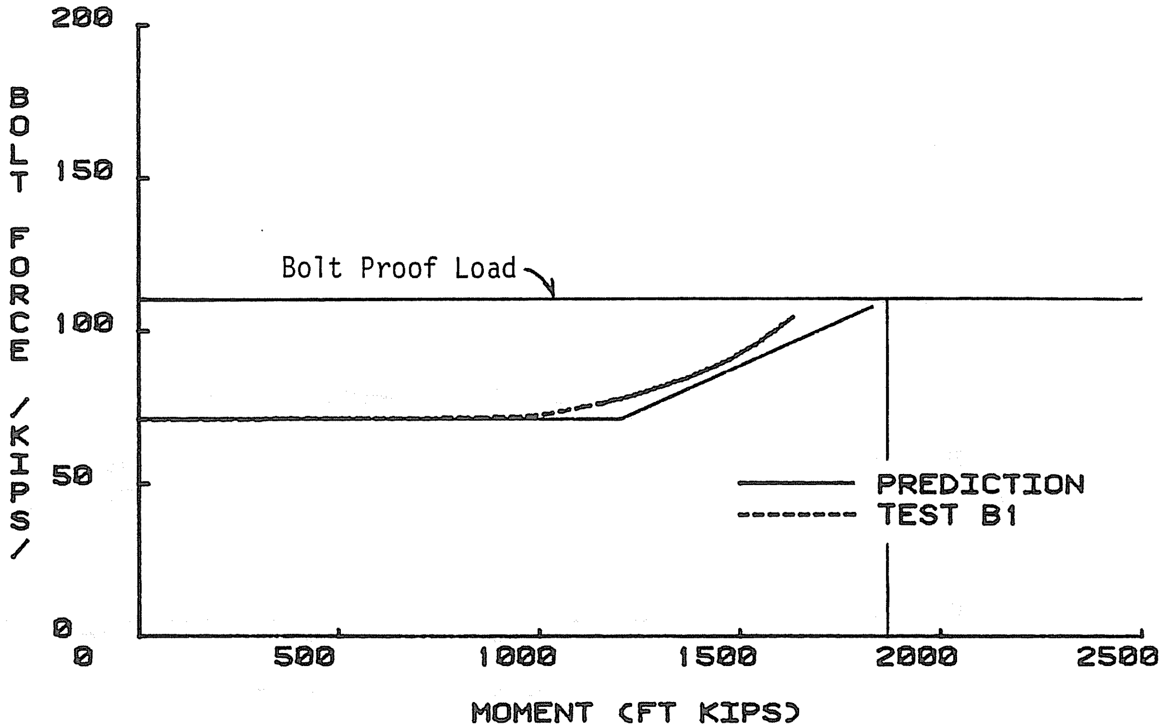

(c) Outer Bolt Force B_1 versus End-Plate Moment

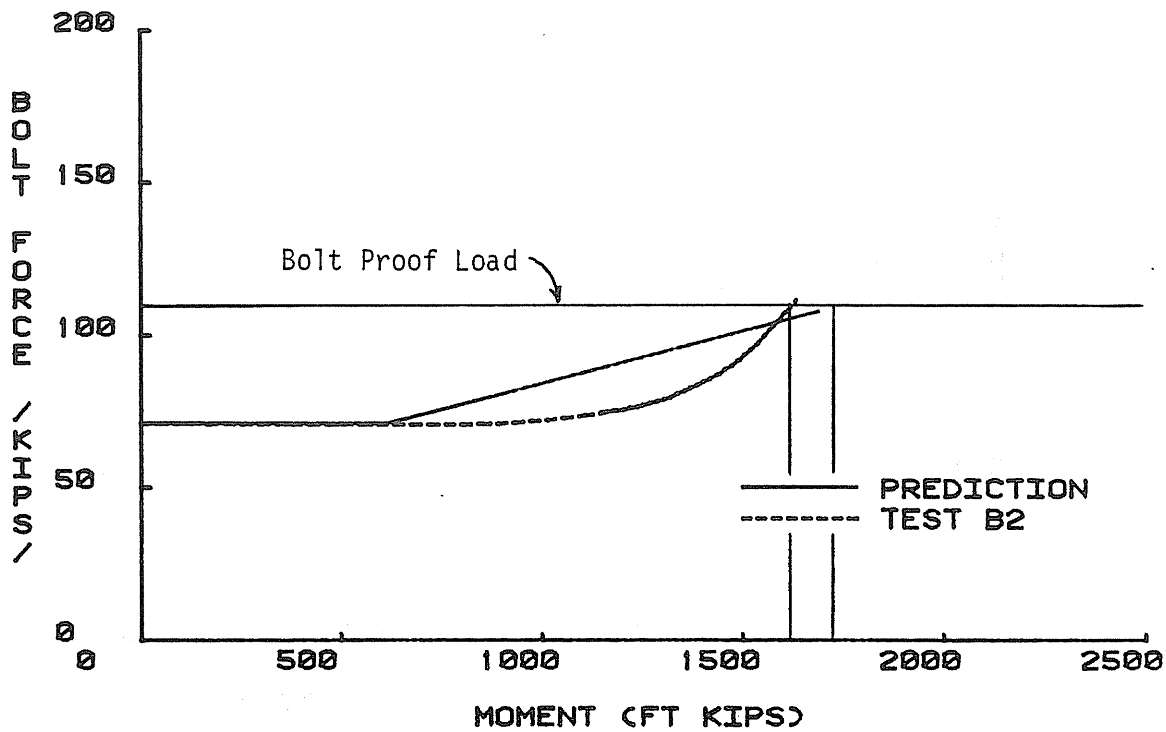

(d) Inner Bolt Force B_2 versus End-Plate Moment

Figure F.1 Results from Test MRE1/3-1 1/4-5/8-62, Continued

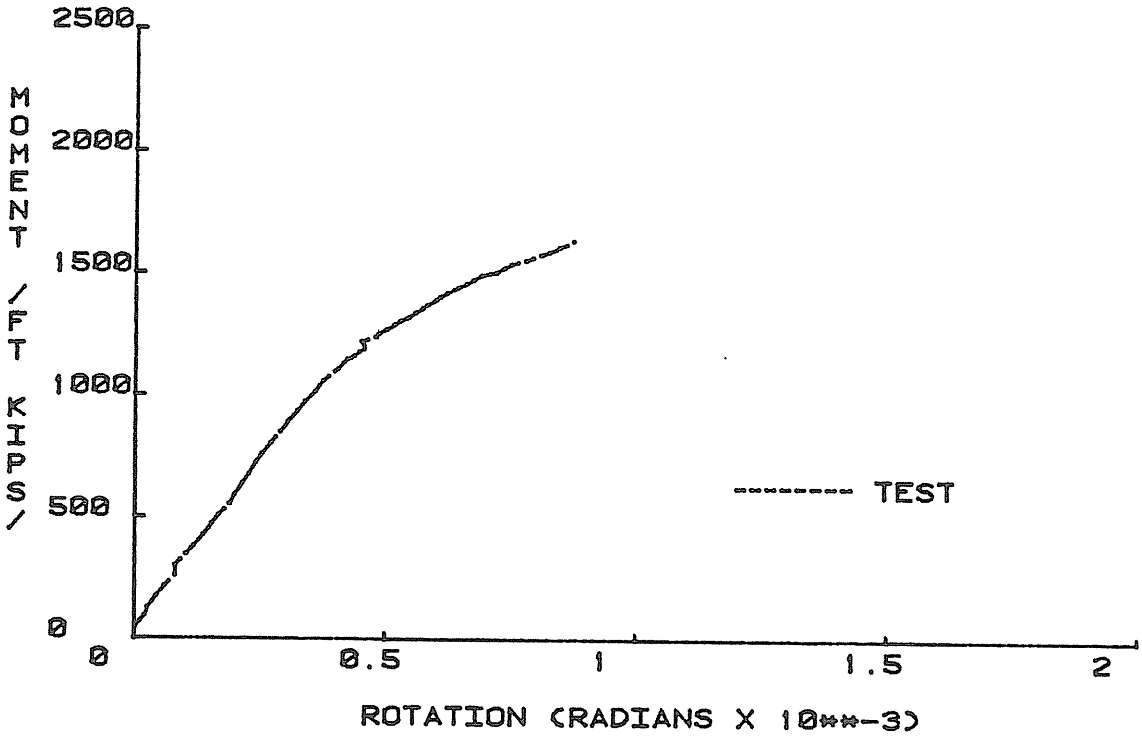

(g) End-Plate Moment versus Rotation

Figure F.1 Results from Test MRE1/3-1 1/4-5/8-62, Continued

APPENDIX G

MRE1/3-1 1/2-3/4-62 TEST RESULTS

TEST SYNOPSIS

PROJECT:	MBMA END-PLATE
TEST:	MRE1/3-1 1/2-3/4-62
TEST DATE:	12-11-85
CONNECTION DESCRIPTION:	Multiple row extended 1/3 moment end-plate with a single row of two bolts outside and three rows of two bolts inside the beam tension flange

BEAM DATA:				
Depth	h	(in)	=	61.945
Flange width	bf	(in)	=	9.926
Web thickness	tw	(in)	=	0.375
Flange thickness	tf	(in)	=	1.005
Moment of inertia	I	(in**4)	=	25,252.9
END-PLATE:				
Thickness	tp	(in)	=	0.753
Extension outside beam flange	pext	(in)	=	5.130
Pitch to bolt from flange	pf	(in)	=	2.584
Pitch between bolt rows	pb	(in)	=	4.516
Gage	g	(in)	=	5.559
Steel yield stress	Fpy	(in)	=	54.6
BOLT DATA:				
Type			=	A325
Diameter	db	(in)	=	1.500
Pretension force	Tb	(k)	=	103.0
PREDICTION:				
End-plate failure moment	Mu	(k-ft)	=	1601.6
Bolt failure (proof) moment	Myb	(k-ft)	=	2575.2
Beam failure moment		(k-ft)	=	3717.8
EXPERIMENTAL:				
Maximum applied moment		(k-ft)	=	2329.6
Moment at bolt proof load		(k-ft)	=	2221.8
Maximum vertical centerline deflection		(in)	=	1.499
Maximum inner end-plate separation		(in)	=	0.0512
Maximum outer end-plate separation		(in)	=	0.1146

DISCUSSION:

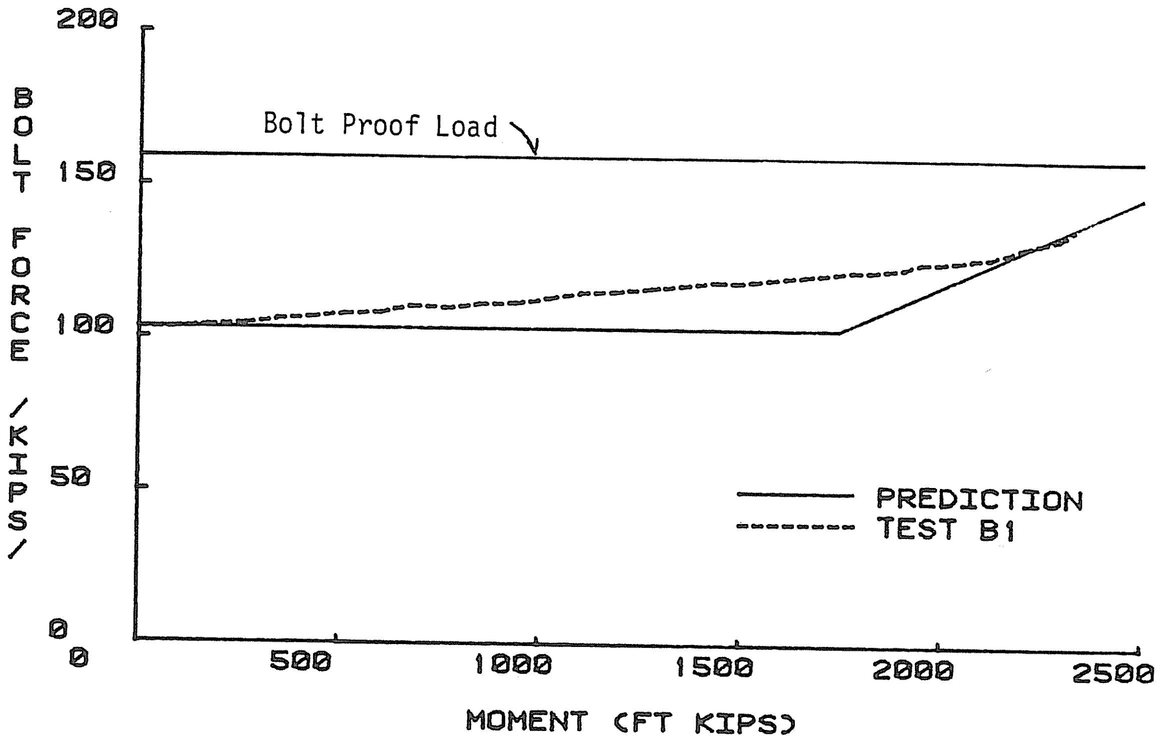

(c) Outer Bolt Force B_1 versus End-Plate Moment

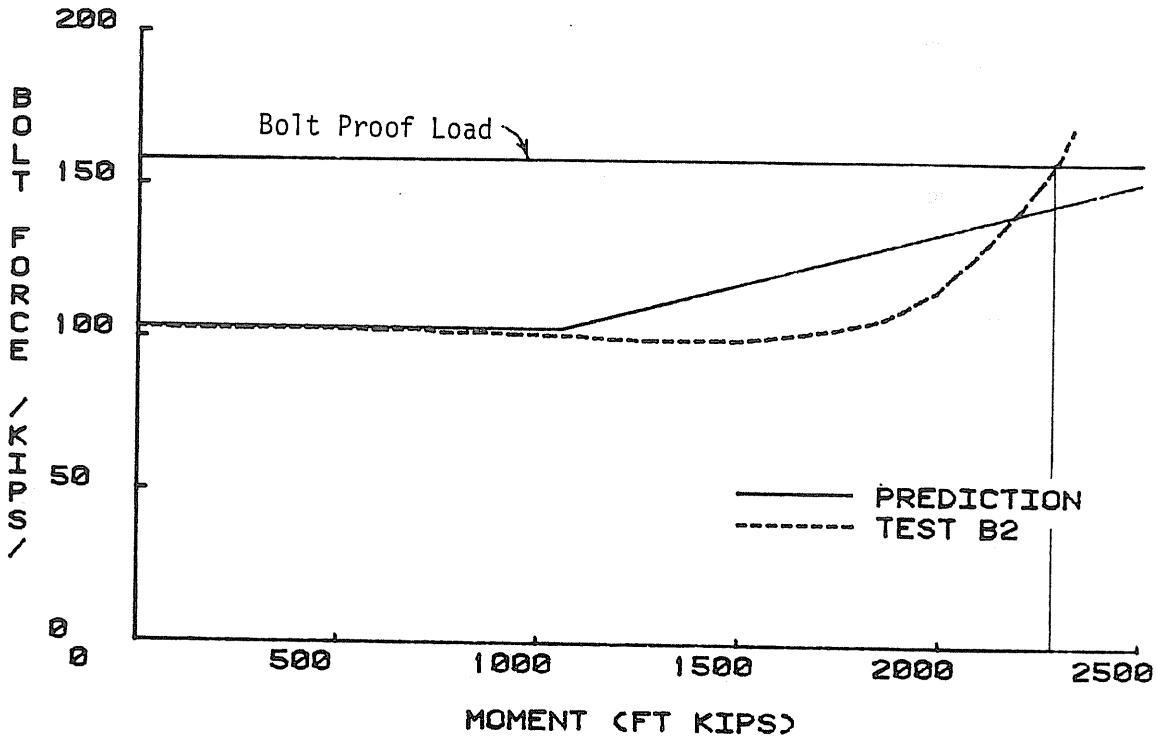

(d) Inner Bolt Force B_2 versus End-Plate Moment

Figure G.1 Results from Test MRE1/3-1 1/2-3/4-62, Continued

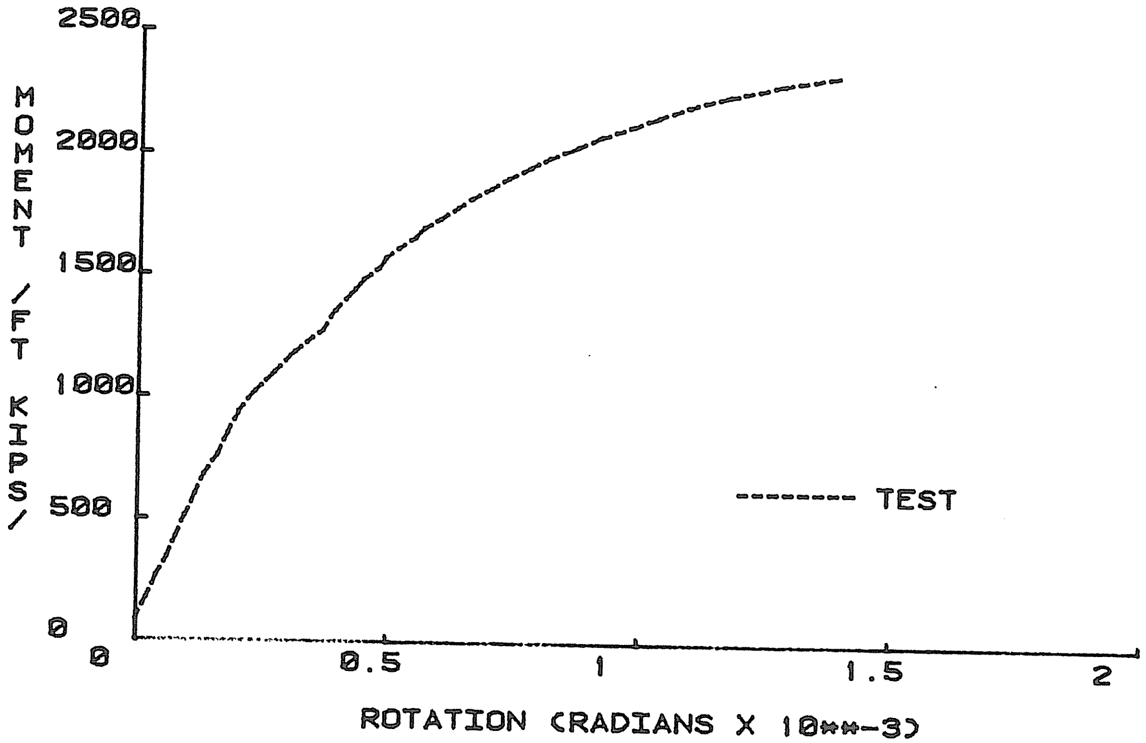

(g) End-Plate Moment versus Rotation

Figure G.1 Results from Test MRE1/3-1 1/2-3/4-62, Continued